博士論文

Rapid Fabrication of Metal Nanostructures by Laser Ablation under Supreme Condition

Mardiansyah Mardis
481612008

化学・生物工専攻　分子化学工学分野

指導教員　後藤元信　神田英輝

平成 30 年度

名古屋大学大学院

Contents

[CHAPTER 1]

Introduction

1-1 Background and Outline of the Thesis

The invention of laser apparatus in the early 1960 allows researchers to exploit its extraordinary characteristic to broad technological applications. One of the applications of laser is on the field of materials processing. It was made possible to evaporate and deposit materials utilizing a more advanced laser-specific irradiation technique, namely the pulsed laser ablation (PLA) or may also be referred as pulsed laser deposition (PLD) in the beginning of its development. The first work on material processing using the PLA technique was conducted by Smith and Turner, who by evaporating some selected solid materials in vacuum tried to deposit the materials [1]. Although at that time they were not able to deposit the materials efficiently compared to the other conventional techniques, such as the chemical deposition, many researchers have since learned the PLA of solid with the progress of cutting edge pulsed laser tools [2].

In the early days of PLA processing on the solid material targets, the experiments were carried out under vacuum condition or in the diluted gas medium, thus the name of PLA/PLD can be specified as one of the physical vapor deposition (PVD) methods. The considered groundbreaking advanced material preparation, for instance, was conducted by irradiation of $YBa_2Cu_3O_{7-x}$ in a small vacuum system with a base pressure of 5×10^{-7} Torr in order to synthesize the Y-Ba-Cu oxide superconductor [3]. In this kind of experiment, the resulting product of laser ablation comes directly from the buildup of

plasma plume produced by the interaction between the laser pulse and the surface of the target. However, apart that the PLA in vacuum presents a versatile method for material preparations, it has disadvantage, mainly the broad distribution of the prepared particle size and concentration, even in the scale of micrometer [4,5]. The disadvantage may cause undesired electronic, magnetic and mechanical properties of the target materials.

On the process development of the material synthesis method employing the PLA, researchers began trying to change the medium to the liquid. In the beginning, the laser irradiation of the solid materials under the liquid media seemed to be less favorable than the application PLA on the gas-solid target. The laser pulse - solid target interaction in liquid media seems to be more complicated than that of in the vacuum or in a gaseous environment. Apart of that, several studies reported the interaction between a laser pulse and a solid target in liquid, whereas its applications on the advanced materials processing were less developed.

The first study of PLA in liquid state was reported in 1987 by Patil et al. [6]. They synthesized metastable iron oxides using PLA with bulk iron target in water. Soon after, Ogale and co-workers published a series of breakthrough works of the unique solid phases produced by laser ablation in the liquid [7–9]. They reported that it was possible to modify the surface properties of metals, oxides and nitrides employing the PLA in liquids while they also observed the diamond phase of carbon generated by irradiating graphite target in benzene liquid.

Since the works by Ogale and co-workers, PLA of solids in liquid have been more attractive for researchers, where there are more possible applications that can be achieved from this technique. For instance, laser can be used to induce surface pattern by employing the wet etching process at the liquid-substrate interface [10,11]. Another

example is that the PLA in liquid can be employed to prepare surface coatings on substrates [12]. Next, the small particulates on the surface can be removed by employing the steam laser cleaning method on the basis of ejection effect of laser irradiation in liquids [13]. Last but not least, a wide array of nanoparticles, nanocrystals and nanostructures have been synthesized by PLA of solid targets in various liquids [14,15].

Nanoparticles, which is synonymous with nanostructure, nanocrystaline, nanophase, among others, may be defined as the particles with the size of below several tens of nanometers. They have totally different chemical and physical properties compared to the bulk phases mainly due to the quantum effects. These unique properties raise the potential application of their usages in the electronic, chemical and mechanical industries for catalysts, drug carriers, sensors, pigments, magnetic and electronic materials.

Among the potentially applicable nanoparticles for science and technology are nickel (Ni), gold (Au), and titania (TiO_2) nanoparticles (NPs). Ni is a known magnetic material in its bulk phase. The nanophase of Ni, which is also magnetic, may hold potential technological applications in industrial scale, such as for chemical catalysis [16]. Gold nanoparticles (Au-NPs) is one of the most extensively nanoparticles studied. Au-NPs unique chemical properties allow their application as catalysts [17] where depending on the size, larger gold particles show less catalytic activity compared to the smaller gold nanoparticles. For such a metal, bulk gold is usually considered as inactive catalyst. One of the remarkable properties of gold nanoparticles is their optical property due to localized surface plasmon resonance (LSPR). The main application of LSPR in gold nanoparticles is in the field of biophysics where they can be used as biomolecule sensors, bio-imaging for cancer treatment and photothermal cancer

therapy [18]. Au-NPs deposited on titania (TiO_2) nanosystem, dubbed as Au/TiO_2 composite nanoparticles even show greater potential promising application in the daily life. Owing the high photocatalytic [19] and antibacterial [20,21] activity properties of TiO_2, the composite NPs are very useful to both convert the chemical pollutants into the less hazardous chemicals [22] and kill the harmful bacteria in water [20].

Owing the versatility of the material synthesis by the PLA technique, our group has begun to experiment to synthesize NPs using the PLA since 2011. Goto and co-workers [23–25] were pioneering this type of research by synthesizing Au and Ag NPs by PLA of the pure Au and Ag metal immersed in supercritical CO_2 (SC-CO_2) media. It turned out that the pressure and temperature of the SC-CO_2 have strong effects to the size and shape of the generated nanoparticles. Yet the questions remain: Are there any effects of the different liquid media if we want to synthesize same NPs? Do the generated NPs have uniform composition or not?

1-2 Some Reviews on The Synthesis of Nanoparticles by Laser Ablation

A vast amount of nanocrystals including diamond, carbides and related materials [14,26–29], elemental nanocrystalline [30–36], alloys, oxides, nitrides, among others has been synthesized via laser ablation in liquid media [37,38]. The generated nanocrystals may have phases that cannot be obtained by conventional synthetic routes. Besides, the thermodynamically stable or kinetically inert phases may be readily converted into more reactive phases. For example, the phase transition from graphite to diamond is well known to take place under extreme pressure and temperature and kinetically unfavorable, as stipulated in the carbon phase diagram.

Ogale et al. reported to have successfully obtained diamond particulates by irradiating pyrolytic graphite target in a benzene solution using the ruby laser [26]. Yang et al. [27,28] and Amans et al. [29] reported the structure and crystalline morphology of the diamond nanocrystals formed by the Nd:YAG laser ablation of an isotopic graphite target in water, acetone, and alcohol.

Reports on the Au-NPs preparation by the PLA from Au plate immersed in pure liquid media such as water [32,34,39–42], *n*-decane [43], dimethylsulfoxide (DMSO), tetrahydrofuran (THF), acetonitrile (ACN) [44], chloroform [45], ethanol [45] and toluene [45,46] are emerging steadily. The Au nanoparticles generated in those media have the size of 1.8 – 18 nm, depending on the laser wavelength, duration and the fluence.

Takada et al. prepared nanocrystalline titanium nitride (Ti_3N_4) NPs by irradiating titanium plate in liquid nitrogen [47]. Zeng et al. prepared hybrid Zn/ZnO core/shell structure NPs by irradiating pristine zinc plate in an aqueous solution with sodium dodecyl sulfate (SDS) as the solute [48]. Hajiesmailbaigi et al has succesfully synthesized Au/TiO_2 nanoparticles by irradiating gold (Au) metal plate in TiO_2 sol solution with Nd:YAG laser at a wavelength of 1064 nm, a repetition rate of 5 Hz, and a pulse width of 20 ns [49].

Hence, these studies demonstrate that laser ablation in liquids could be regarded as an alternative synthetic method of nanomaterials.

1-3 Purpose of this Study

Motivated by these intriguing experiments, the author decided to further elaborate the synthesis of nanoparticles under supercritical media employing the PLA technique

with different liquid media conditions. The works reported in this thesis aim at basic understanding of the mechanisms of PLA under liquid and supercritical CO_2, water and amino acid solvent.

The content is arranged as follows. A brief introduction of laser ablation and its application on the synthesis of nanoparticles is given in Chapter 1. In Chapter 2, 3, 4, 5 and 6, a detailed discussion about this work is given, towards the unique particles generated in liquid and supercritical fluid. Finally, a summary and outline are discussed with regard to the challenges that remain in the field is presented in Chapter 7.

1-4 References

[1] Smith, H. M.; Turner, A. F. *Appl. Opt.* **1965**, *4*, 147.

[2] Greer, J. A. *J. Phys. D. Appl. Phys.* **2014**, *47*.

[3] Dijkkamp, D.; Venkatesan, T.; Wu, X. D.; Shaheen, S. A.; Jisrawi, N.; Min-Lee, Y. H.; McLean, W. L.; Croft, M. *Appl. Phys. Lett.* **1987**, *51*, 619.

[4] Willmott, P. R.; Huber, J. R. *Rev. Mod. Phys.* **2000**, *72*, 315.

[5] Kuppusami, P.; Raghunathan, V. S. *Surf. Eng.* **2006**, *22*, 81.

[6] Patil, P. P.; Phase, D. M.; Kulkarni, S. A.; Ghaisas, S. V.; Kulkarni, S. K.; Kanetkar, S. M.; Ogale, S. B. *Phys. Rev. Lett.* **1987**, *58*, 238.

[7] Ogale, S. B. *Thin Solid Films* **1988**, *163*, 215.

[8] Ogale, S. B.; Patil, P. P.; Roorda, S.; Saris, F. W. *Appl. Phys. Lett.* **1987**, *50*, 1802.

[9] Ghaisas, S. V.; Malshe, A. P.; Patil, P. P.; Kanetkar, S. M.; Ogale, S. B.; Bhide, V. G. *J. Appl. Phys.* **1987**, *62*, 2799.

[10] Wang, J.; Niino, H.; Yabe, A. *Appl. Phys. A Mater. Sci. Process.* **1999**, *69*, 271.

[11] Shafeev, G. A.; Obraztsova, E. D.; Pimenov, S. M. *Appl. Phys. A* **1997**, *65*, 29.

[12] Yang, G. W. *Prog. Mater. Sci.* **2007**, *52*, 648.

[13] Zapka, W.; Ziemlich, W.; Tam, A. C. *Appl. Phys. Lett.* **1991**, *58*, 2217.

[14] Wang, C. X.; Liu, P.; Cui, H.; Yang, G. W. *Appl. Phys. Lett.* **2005**, *87*, 1.

[15] Yang, L.; May, P. W.; Yin, L.; Smith, J. A.; Rosser, K. N. *Diam. Relat. Mater.* **2007**, *16*, 725.

[16] Lewis, L. N. *Chem. Rev.* **1993**, *93*, 2693.

[17] Bond, G. C.; Louis, C.; Thompson, D. T. *Catalysis by Gold*; Imperial College Press: London, 2006.

[18] Louis, C.; Pluchery, O. *Gold Nanoparticles for Physics, Chemistry and Biology*; Imperial College Press: London, 2012.

[19] Li, H.; Bian, Z.; Zhu, J.; Huo, Y.; Li, H.; Lu, Y. **2007**, No. 101, 4538.

[20] Armelao, L.; Barreca, D.; Bottaro, G.; Gasparotto, A.; Maccato, C.; Maragno, C.; Tondello, E.; Štangar, U. L.; Bergant, M.; Mahne, D. *Nanotechnology* **2007**, *18*, 375709.

[21] Fu, G.; Vary, P. S.; Lin, C.-T. *J. Phys. Chem. B* **2005**, *109*, 8889.

[22] Ayati, A.; Ahmadpour, A.; Bamoharram, F. F.; Tanhaei, B.; Mänttäri, M.; Sillanpää, M. *Chemosphere* **2014**, *107*, 163.

[23] Machmudah, S.; Goto, M.; Wahyudiono; Kuwahara, Y.; Sasaki, M. *Res. Chem. Intermed.* **2011**, *37*, 515.

[24] Machmudah, S.; Wahyudiono; Kuwahara, Y.; Sasaki, M.; Goto, M. *J. Supercrit. Fluids* **2011**, *60*, 63.

[25] Machmudah, S.; Sato, T.; Kuwahara, Y.; Sasaki, M.; Goto, M. *Trans. Mater. Res. Soc. Japan* **2011**, *36*, 465.

[26] Ogale, S. B.; Malshe, A. P.; Kanetkar, S. M.; Kshirsagar, S. T. *Solid State Commun.* **1992**, *84*, 371.

[27] Yang, G. W.; Wang, J. B. *Appl. Phys. A* **2000**, *71*, 343.

[28] Yang, G. W.; Wang, J. Bin; Liu, Q. X. *J. Phys. Condens. Matter* **1998**, *10*, 7923.

[29] Amans, D.; Chenus, A. C.; Ledoux, G.; Dujardin, C.; Reynaud, C.; Sublemontier, O.; Masenelli-Varlot, K.; Guillois, O. *Diam. Relat. Mater.* **2009**, *18*, 177.

[30] Švrček, V.; Kondo, M. *Appl. Surf. Sci.* **2009**, *255*, 9643.

[31] Intartaglia, R.; Bagga, K.; Scotto, M.; Diaspro, A.; Brandi, F. *Opt. Mater. Express* **2012**, *2*, 510.

[32] Sylvestre, J.; Poulin, S.; Kabashin, A. V; Sacher, E.; Meunier, M.; Luong, J. H. T.; Montre, Ä. P. De; Postale, C. *J. Phys. Chem. B* **2004**, *108*, 16864.

[33] Sylvestre, J. P.; Kabashin, A. V.; Sacher, E.; Meunier, M.; Luong, J. H. T. *J. Am. Chem. Soc.* **2004**, *126*, 7176.

[34] Mafuné, F.; Kohno, J.; Takeda, Y.; Kondow, T.; Sawabe, H. *J. Phys. Chem. B* **2001**, *105*, 5114.

[35] Imam, H.; Elsayed, K.; Ahmed, M. A.; Ramdan, R. *Opt. Photonics J.* **2012**, *2*, 73.

[36] Tilaki, R. M.; Iraji zad, A.; Mahdavi, S. M. *Appl. Phys. A* **2007**, *88*, 415.

[37] Amendola, V.; Meneghetti, M. *Phys. Chem. Chem. Phys.* **2009**, *11*, 3805.

[38] Zeng, H.; Du, X. W.; Singh, S. C.; Kulinich, S. A.; Yang, S.; He, J.; Cai, W. *Adv. Funct. Mater.* **2012**, *22*, 1333.

[39] Petersen, S.; Barchanski, A.; Taylor, U.; Klein, S.; Rath, D.; Barcikowski, S. *J. Phys. Chem. C* **2011**, *115*, 5152.

[40] Kabashin, A. V.; Meunier, M. *J. Appl. Phys.* **2003**, *94*, 7941.

[41] Besner, S.; Kabashin, A. V.; Meunier, M. *Appl. Phys. A Mater. Sci. Process.* **2007**, *88*, 269.

[42] Compagnini, G.; Messina, E.; Puglisi, O.; Nicolosi, V. *Appl. Surf. Sci.* **2007**, *254*, 1007.

[43] Compagnini, G.; Scalisi, A. A.; Puglisi, O. *J. Appl. Phys.* **2003**, *94*, 7874.

[44] Amendola, V.; Polizzi, S.; Meneghetti, M. *J. Phys. Chem. B* **2006**, *110*, 7232.

[45] Nikov, R. G.; Nedyalkov, N. N.; Atanasov, P. A.; Karashanova, D. B. *Appl. Phys. A Mater. Sci. Process.* **2017**, *123*, 1.

[46] Amendola, V.; Rizzi, G. A.; Polizzi, S.; Meneghetti, M. *J. Phys. Chem. B* **2005**,

109, 23125.

[47] Takada, N.; Sasaki, T.; Sasaki, K. *Appl. Phys. A Mater. Sci. Process.* **2008**, *93*, 833.

[48] Zeng, H.; Li, Z.; Cai, W.; Cao, B.; Liu, P.; Yang, S. *J. Phys. Chem. B* **2007**, *111*, 14311.

[1] [49] Hajiesmaeilbaigi, F.; Motamedi, A.; Ruzbehani, M. *Laser Phys.* **2009**, *20*, 508.

[CHAPTER 2]

Nickel Nanoparticles Generated by Pulsed Laser Ablation in Liquid CO_2

Abstract

Nickel nanoparticles with various structures were synthesized by a pulsed laser ablation (PLA) process in liquid CO_2 at 17°C and 5.2 MPa. A nickel plate immersed in liquid CO_2 was subjected as a target. This was irradiated by a laser beam with a fundamental wavelength of 1064 nm at 2.46 mJ for 15 min. The generated particles were deposited on a silicon wafer after natural evaporation of the liquid CO_2, and analyzed by field emission scanning electron microscopy (FE-SEM), scanning electron microscopy with energy-dispersive X-ray spectroscopy (SEM/EDS), and transmission electron microscopy (TEM). Nickel and carbon particles with sphere-like structures or apple-shaped structures were observed. Furthermore, characteristic nickel/carbon particles with core/shell structures were also produced. The generated particles ranged in size between 5–350 nm in diameter, with dominant sizes under 50 nm.

2-1. Introduction

Nanoscience has recently attracted much attention from researchers due to the unique properties of nanomaterials. At small scales, materials gain interesting physical and chemical phenomena which can be exploited in various technological fields such as medicine, catalysis, and electronic devices [1-7]. Hence, a simple, efficient, and

eco-friendly method for synthesizing nanoparticles is necessary [8-9]. Pulsed laser ablation (PLA) is an interesting method to synthesize nanoparticles. The advantages of PLA include the ability to synthesize particles from any solid material, the generation of high-purity particles, and short particle formation times [11-14]. Usually, PLA is performed under vacuum [15-18]. In vacuum conditions, laser irradiation at UV wavelengths can lead to a remarkable change in the size distribution of nickel particles [17]. A thin film of silver particles can also be synthesized by PLA in vacuum [15]. Ou et al. [18] conducted a one-step synthesis method of carbon encapsulated nickel nanoparticles using a long pulse laser to ablate a nickel target in methane or mixture of methane and helium at room temperature. They reported that carbon encapsulated metal nanoparticles are easy to produce by long pulse laser ablation method in wide range of methane/helium mixture pressure and methane concentration. In this synthesis method, the synthesis chamber was evacuated to a base pressure of 5 Pa before experiment. Roy et al. [10] also performed metal nanoparticles deposited on few-layered graphene using pulsed laser ablation catalyze the in-situ formation of graphitic shells from graphene. They were able to synthesize core–shell nanoparticles directly from few layered graphene using a one-step pulsed laser deposition based process and reported that the cores consisted of metal nanoparticles. All depositions were done at a pressure 4×10^{-5} mbar. However, in order to use this method, complicated systems with expensive vacuum apparatus are necessary.

Recently, a liquid phase was used as a new synthesis medium for fabricating nanoparticles by PLA [6,7,19-26]. Nanoparticles of nickel and cobalt have been produced via PLA in an organic solution [19]. The formations of titanium, silica, silver, and gold nanoparticles by laser ablation of metal targets in liquid environments have

also been reported [20,21]. This technique has attracted much attention because of its simple process and lack of expensive vacuum equipment. Furthermore, liquid-phase PLA permits the collection synthesized nanoparticles much more easily than PLA in vacuum. Many researchers have reported the formation of unique nanoparticles by changing the liquid medium or by adding some chemical compounds into the medium [22,23,25,27]. Namely, this superimposes the chemical reactivity of the liquid onto the physical process of laser ablation. For instance, in liquid nitrogen, crystalline titanium nitride particles were synthesized [22]. In an aqueous solution with sodium dodecyl sulfate (SDS), Zn/ZnO core/shell nanoparticles were generated [23]. Although the mechanism remains unclear regarding the interaction of active metals from the target in a liquid medium with atoms or molecules from the liquid, the final synthesized products are found to strongly depend on the constituents of the solution involved [24]. Barcikowski [7] stated that laser ablation and nanoparticle generation in liquids has fulfilled this prospect and has been applied to generate, excite, fragment, and conjugate elemental, nanoalloy, semiconductor, or ceramic nanoparticles in the past decade. He also expressed that a huge variety of materials synthesized by pulsed laser ablation in liquids has been presented, from metals to photoluminescent, carbon, or ceramic materials. Here, we focused on the use of liquid CO_2 as a medium. Since the liquid CO_2 includes many carbon atoms, the characteristics of the synthesized particles are expected to include carbon atoms. PLA in liquid CO_2 has not been thoroughly investigated yet. This work may provide important information on the composite products of metal from a metal target and carbon from the liquid medium without added chemical reagents.

PLA in a liquid medium also provides the ability to easily control the size and shape of the produced nanoparticles [28-31]. PLA of a tin target in an ethanol solution of thioacetamide was reported to produce hollow tin monosulfide nanoparticles after acid etching was employed [32]. In this work, PLA with 1064 nm was conducted with a nickel plate as the target in liquid CO_2. The generation of particles composed of nickel and carbon atoms was demonstrated in the study. The morphology, structure, elemental composition, and particle size distribution of the generated particles would be discussed here. Previously, Machmudah et al. [11,12,33] conducted pulse laser ablation under dense CO_2 to generate nanoparticles with gold and silver plates as the target. They reported that gold and silver nanoparticles has been produced with laser wavelength 532 nm. However, the atomic compositions of nanoparticles products were not reported. Generally, the different applied laser wavelength between 1064 and 532 nm would affect on the nanoparticles distributions formed. The nanoparticles distributions of 1064 nm are more homogenous and the average size of nanoparticles prepared at 532 nm is smaller than that prepared at 1064 nm [34].

2-2 Experimental

2-2-1 Materials

A 1-mm-thick nickel plate with an area of 10 × 10 mm, purchased from Nilaco Co., Japan, was employed as a target. A silicon wafer for the collection of synthesized nanoparticles was also purchased from Nilaco Co., Japan. Liquid CO_2 (99.95%) as the PLA medium was supplied by Sogo Co., Japan.

2-2-2 Experimental setup and methods

A schematic of the PLA system for generating nanoparticles in liquid CO_2 is shown in Fig. 1.

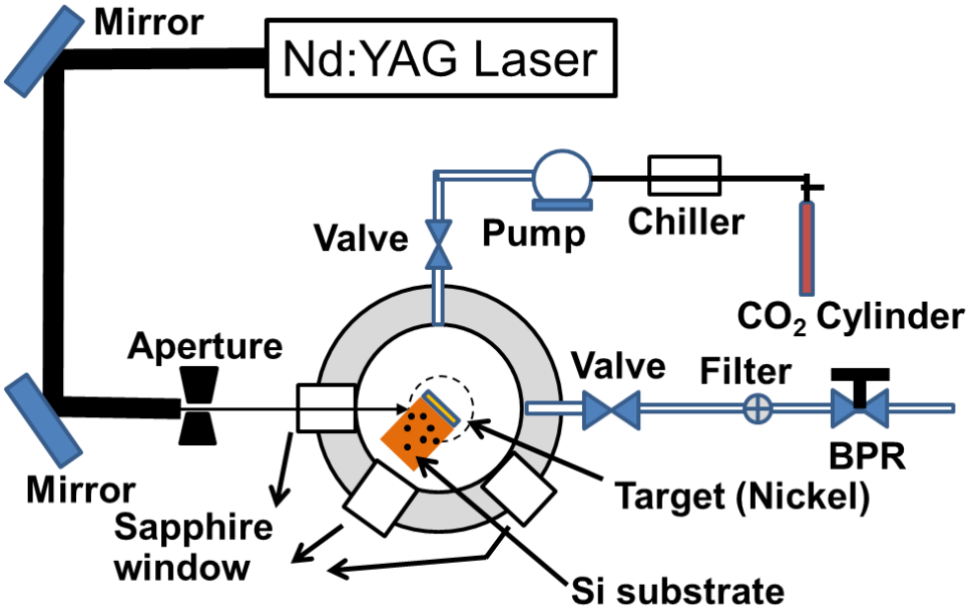

Figure 1. Schematic of PLA system.

Laser pulses from a high-power Q-switched pulsed Nd:YAG laser (Spectra-Physics Quanta-Ray INDI-40-10), with wavelength of 1064 nm, pulse energy of 2.64 mJ, pulse rate of 10 Hz, and pulse duration of approximately 8 ns, were used for ablation. The nickel target was placed at the center of a high-pressure chamber made of SUS 316 stainless steel (110 mL volume, AKICO, Japan) and the Nd:YAG laser was located approximately 1 m from the target. To collect the generated nanoparticles, the silicon wafer was fixed below the target plate. Liquid CO_2 was pressurized and pumped into the chamber using a high-performance liquid chromatography (HPLC) pump (PU-1586, Jasco Co., Japan). The chamber temperature was regulated with a temperature controller and the pressure was controlled with a back-pressure regulator.

The temperature and pressure for the experiments were 17.0℃ and 5.2 MPa, respectively. A thermocouple for monitoring the experimental temperature was inserted into the chamber. K-type thermocouples were also inserted into the chamber's walls to measure the radial temperature distribution. After the set pressure and temperature were reached, PLA was performed for 15 min. The particles deposited on the silicon wafer were collected after natural evaporation of the liquid CO_2, and then analyzed by FE-SEM (Model JSM-6330F, JEOL, Japan). SEM/EDS observations (Model JED-2140GS JEOL, Japan) were also performed to determine the products' elemental composition. Transmission electron microscopy (TEM) was carried out on a Hitachi H9000NAR microscope equipped with a cold field-emission gun. The acceleration voltage was 300 kV, and the TEM images were captured by CCD (charge-coupled device) camera. The specimens were prepared by the following procedure: the sample was ultrasonically dispersed in ethanol for 15 min, then a drop of sample was loaded onto the copper grid and stored in desiccator overnight at room temperature to desorb atmospheric contaminants. The size of particles was measured by using image analyzer software (Image J 1.42).

2-3 Results and Discussion

FE-SEM images of the nanoparticles generated by exposure to the Q-switched Nd:YAG pulsed laser beam at 17.0 ℃ and 5.2 MPa for 15 min are shown in Fig. 2.

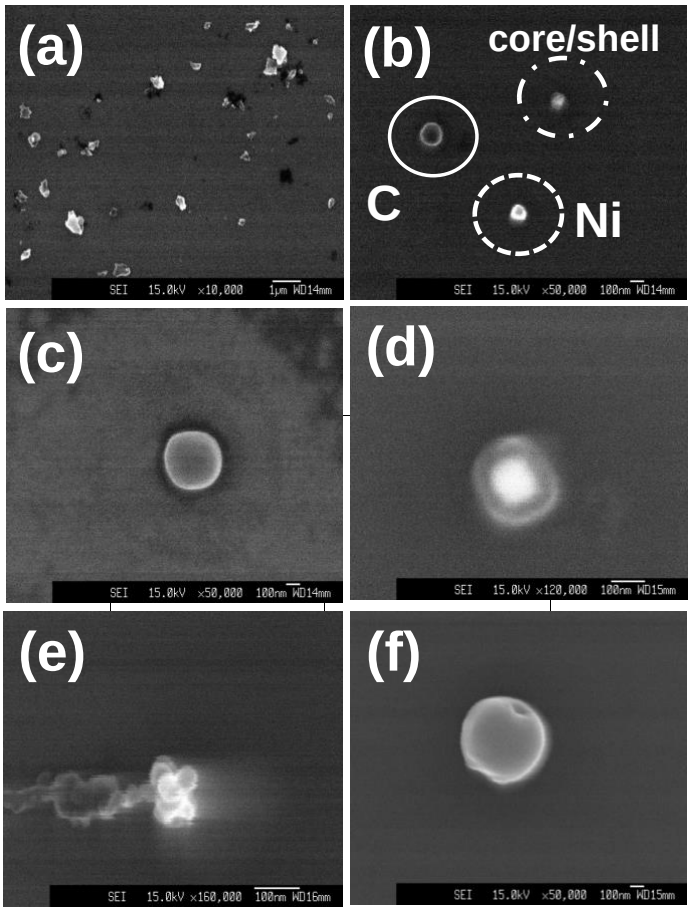

Figure 2. SEM images of nanoparticles synthesized using PLA in liquid CO_2.

As shown at low magnification in Fig. 2(a), the collected particles are spread on the silicon wafer with particle sizes under 1 μm, and both spherical and irregular in shape. Since the size of the irregular particles is approximately 500–1000 nm, impurities are assumed to have entered from the chamber wall and the target. These irregular particles are considered not to be the generated target particles and are excluded from our evaluation in this work. The observation of particles at higher magnification, shown in Fig. 2(b), clarifies the existence of spherical particles with three characteristic types and different contrasts. We observe the first type as white color particles. Particles appearing white in SEM images are known to usually be metal

particles. Therefore, we considered the white color particles to be metal; in this case, they might be nickel nanoparticles [35], as indicated by the dashed circle in Fig. 2(b). Cui et al. [35] informed that under the electron beam of SEM with aluminium sample holder, nickel and aluminum show very different contrast with nickel appearing white color and aluminum showing dark color. This helps us discern the two materials under high magnification SEM imaging. Additionally, based on the examination results of SEM/EDS on the area, nickel's atomic signals were detected. The second type is ring-like particles, indicated by the solid-line circle in Fig. 2(b). A larger particle of the same type is also shown in Fig. 2(c). From SEM/EDS results for this particle, the atomic compositions of carbon, oxygen and nickel are 99%, 1% and 0%, respectively. We suggest that this ring-like particle shown in Fig. 2(c) is a spherical carbon nanoparticle. Namely, PLA in liquid CO_2 can generate carbon nanoparticles, in addition to the target materials. Due to the high density of liquid CO_2 (920.3 kg/m^3) and the high-temperature plasma plume (8000 K) induced at the vicinity of the metal target [36,37], molecular CO_2 may decompose into carbon nanoparticles. Niu et al. [38] explained that when the PLA was applied to the metal target in a liquid medium, the local area around the laser spot melts to generate a primary metal nanodroplet first. Due to the liquid confinement on the metal target, the applied laser irradiation will boil the surrounding liquid medium and generates high-pressure vapor. The hot metal nanodroplets react with the liquid medium gradually via their surfaces. The degree and rate of such reactions on the metal nanodroplet surface were primarily controlled by the liquid reactivity and the applied laser irradiation parameters, thus leading to products with different morphologies and chemical compositions. The third type of particle is those with core/shell-like structures, enclosed by the dash-dot circle in Fig. 2(b) and

expanded in Fig. 2(d). The center area is white and spherical, approximately 100 nm in diameter. The outer area is covered by a ring-like structure with a thickness of approximately 50 nm. To examine the particle's features more clearly, the atomic composition was investigated by SEM/EDS, as shown in Fig. 3. The composition was investigated based on the core, shell, and outer surface of the particle. The results are summarized in Fig. 3.

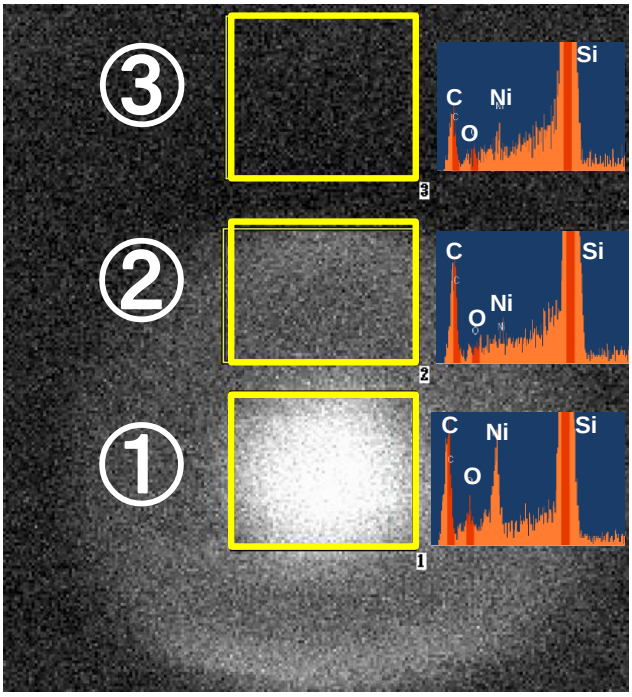

Area	C	O	Ni
1	88.8	5.8	5.4
2	99.8	0	0.2
3	97.7	2.3	0

Figure 3. SEM/EDS examination results of a synthesized core/shell particle.

Notably, the core area of the particle, area 1, has the largest content of nickel (5.4%) compared with other areas. The core is suggested to be a nickel-rich particle. However, 5.8% oxygen atoms were also included in this area. Therefore, we consider the possibility of a nickel-oxygen or carbon-oxygen layer in the core area of the particle. In the shell area, nickel and oxygen levels are very low, allowing the dominance of carbon (99.8%). According to these results, it could be said that the nanoparticle shown in Fig. 2(d) possesses a nickel/carbon core/shell structure. Since the liquid used in PLA is CO_2, the decomposition to elemental carbon and oxygen in high-temperature plasma occurs. As a result, carbon shells form which enclose the nickel nanoparticles. The formation of the nickel/carbon core/shell nanoparticles obtained from PLA may be explained by nucleation and growth mechanisms. After the laser energy is absorbed by the nickel plate, the high-temperature plasma plume forms at the solid-liquid interface. When the temperature and pressure of the plasma plume decrease, the metal vapor ions condense rapidly to form nickel particles. Similar to the laser ablation of toluene [39], the breakdown of liquid CO_2 in the vicinity of the target may occur simultaneously, which produces highly active carbon atoms as well as carbon chains. The active carbon atoms polymerize to form carbon layers surrounding the nickel nanoparticle core. The core/shell structure also resulted from PLA in liquid toluene with a cobalt target [39]. In addition, the formation of core/shell nanoparticles using metals such as gold, silver, and iron oxide have been reported [40,41]. Even though the carbon shell shown in this paper is unusual, it has many advantages regarding the simple and versatile technique without added chemical reagents. Carbon is stable even under harsh application conditions, such as in very high or low pH, and may effectively protect the core materials from environmental degradation, as well as hinder the aggregation of neighboring particles.

Carbon's good electric conduction can overcome the limitation of insulator coatings in biosensor and fuel-cell applications. Various functional groups (such as –OH and -COOH) can be added to the carbon surface by oxidation, profoundly enhancing the dispersibility of the nanoparticles in polar solutions. Functional groups on the carbon layer can be utilized to obtain ternary hybrid structures. Therefore, it is of great significance that PLA in liquid CO_2 can form carbon-shell structures on core materials.

The aggregated nanoparticles with lengths of approximately 300–400 nm are also observed, as depicted in Fig. 2(e). This shows that the aggregation of nickel particles connects to the aggregation of carbon particles. However, under liquid CO_2, small particles attached in sphere-like agglomerates could not be observed with the specificity available to particles generated under supercritical CO_2 [33]. This may be due to the changed CO_2 density. The network structure of agglomerated particles may change the properties of the nickel nanoparticles [33].

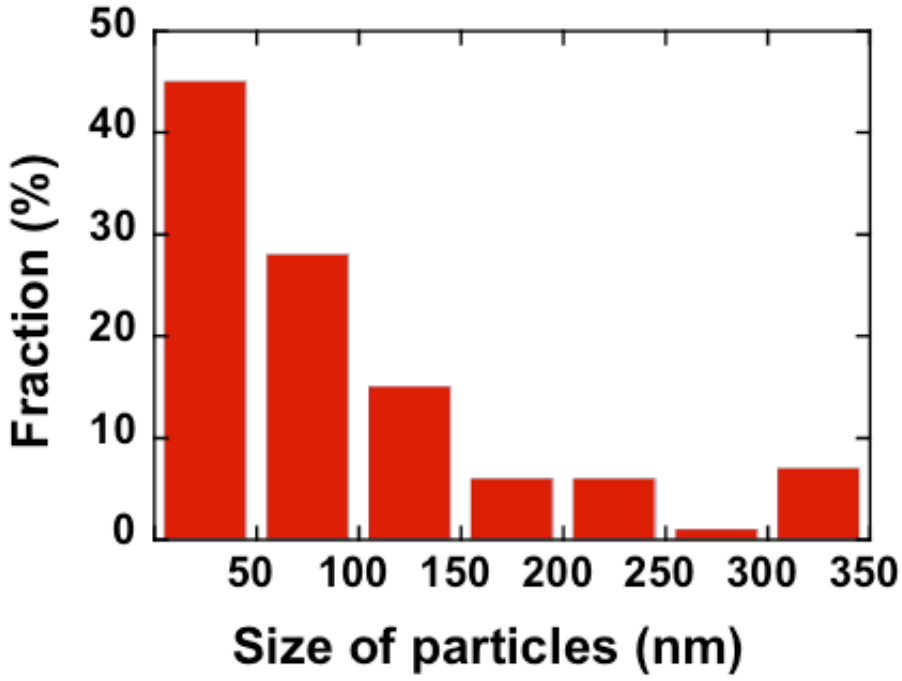

Figure 4. Size distribution of particles synthesized by PLA in liquid CO_2.

The agglomeration phenomenon may occur due to the dense environment, which can hasten coagulation and quenching of the metal atoms. The medium adjacent to the laser-ablated area of the target contains a significant number of nanoclusters, favoring their growth and the formation of a networked structure [42]. The apple-like nanoparticles were also observed in this study, as shown in Fig. 2(f). This is known to be the shape of hollow particles [32]. The formation of hollow nanoparticles can be explained by two possible causes. The laser beam's contact may have generated these particles [24]; alternately, the pressure change may have induced cavitation bubbles on the surface of metal target. These cavitation bubbles would change to liquid bubbles without pressure changes in the neighborhood of CO_2's boiling temperature [43]. Therefore, in our experimental condition (5.0 MPa and 17 ℃), we considered the hollow particles not to be formed by cavitation pressure changes, but by direct laser beam irradiation. Finally, the estimated generated particles' size distribution, measured from the images (at least 200 different particles were randomly selected), is shown in Fig. 4. The particles range in size from approximately 5 to 350 nm. Notably, most particles formed with diameter sizes under 50 nm; and fewer particles are observed at larger particle sizes.

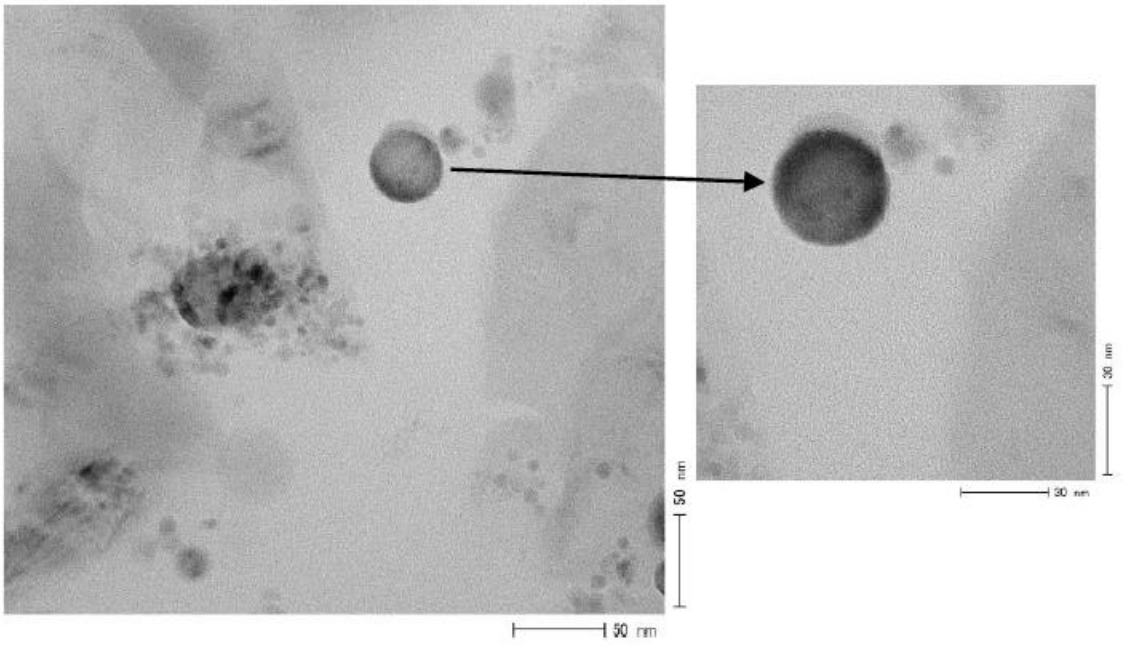

Figure 5. TEM images of nanoparticles synthesized using PLA in liquid CO_2.

It was well known that the characterization of composite materials on a nanometer scale is very important for all types of materials. The TEM is a tool that is capable of showing magnified images of a thin specimen, typically with a magnification in the range 10^3 to 10^6. Figure 5 showed representative TEM images of nickel nanoparticles synthesized in spherical shape. It could be seen that the nickel nanoparticles is embedded in a matrix of carbon. Apparently, this figure shows that nickel nanoparticles consisted of particles with the size around 40 nm with the thickness of the carbon layers coating the core particles around 4 nm. This result is in agreement with the previous research in which metal coated particles were covered by 2-5 nm thin carbon layers [44-46]. Luo et al. [44] conducted experiment for carbon-encapsulated nickel or cobalt nanoparticles by a detonation method using a home-made water-soluble composite explosive. They reported that the detonation products contain face-centered cubic cobalt/nickel nanocrystals approximately 10–25 nm in size, which are encapsulated by thin (3–5 nm) carbon layers. Li et al. [46] also demonstrated a facile

solution method for direct growth of mesoporous carbon-coated nickel nanoparticles on conductive carbon blacks treated carbon fibers, using an oleate-assisted deposition/calcinations process. They obtained the composite product has a uniform nickel core and a carbon surface layer of around 2 nm, which avoids aggregation and pulverization of inner nanoparticles and serves as a protective layer of nickel cores from dissolution during electrochemical reactions. Judging by the result, it could be said that nickel nanoparticles has been synthesized in spherical shape using PLA under liquid CO_2 environment.

2-4 Conclusions

PLA of a nickel plate in liquid CO_2 synthesized various structures of carbon, nickel, and nickel/carbon core/shell particles. The PLA experiments were conducted at temperature of 17.0 ℃ and pressure of 5.2 MPa. SEM images showed that nanoparticles has been generated in spherical morphology. The SEM/EDS results showed that the atomic compositions of carbon, oxygen and nickel are 99%, 1% and 0%, respectively. The SEM/EDS results showed that the particle consisted of atomic carbon, oxygen, and nickel. The size distribution of the synthesized nanoparticles was between 5-350 nm. Based on the results, it is proposed that this method is applicable as a medium for synthesized nanoparticles owing to the simple process by this technique.

2-5 References

[1] M. Daniel, D. Astruc, Chem. Rev. **104,** 293 (2004).

[2] P. K. Jain, K. S. Lee, I. H. El-Sayed, M. A. El-Sayed, J. Phys. Chem. B **110,** 7238 (2006).

[3] C. Estournés, T. Lutz, J. Happich, T. Quaranta, P. Wissler, J. L. Guille, Magnet. Mater. **173**, 83 (1997).

[4] J. Park, E. Kang, S. U. Son, H. M. Park, M. K. Lee, J. Kim, K. W. Kim, H.-J. Noh, J.-H. Park, C. J. Bae, J.-G. Park, T. Hyeon, Adv. Mater. **17,** 429 (2005).

[5] P. V. Kamat, J. Phys. Chem. B **106,** 7729 (2002).

[6] G. W. Yang, Prog. Mater Sci. **52**, 648 (2007).

[7] S. Barcikowski, F. Mafune, J. Phys. Chem. C **115**, 4985 (2011).

[8] S. Kanchi, G. Kumar, A.-Y. Lo, C.-M. Tseng, S.-K. Chen, C.-Y. Lin, T.-S. Chin, Arabian J. Chem. **27,** In Press (2014), doi:10.1016/j.arabjc.2014.08.006.

[9] O. V. Kharissova, H. V. Rasika Dias, B. I. Kharisov, B. O. Perez, V. M. Jimenez Perez, Trends Biotechnol. **31,** 240 (2013).

[10] S. Roy, R. Bajpai, N. Koratkar, D. S. Misra, Carbon **85**, 406 (2015).

[11] S. Machmudah, T. Satoh, Wahyudiono, M. Sasaki, M. Goto, High Press. Res. **32,** 60 (2012).

[12] S. Machmudah, M. Goto, Wahyudiono, Y. Kuwahara, M. Sasaki, Res. Chem. Intermed. **37,** 515 (2011).

[13] S. Wei, T. Yamamura, D. Kajiya, K. Saitow, J. Phys. Chem. C **116**, 3928 (2012).

[14] T. Kato, S. Stauss, S. Kato, K. Urabe, M. Baba, T. Suemoto, K. Terashima, Appl. Phys. Lett. **101**, 224103 (2012).

[15] J. C. Alonso, R. Diamant, P. Castillo, M. C. Acosta–García, N. Batina, E. Haro-Poniatowskilaser, Appl. Sur. Sci. **255,** 4933 (2009).

[16] S. Amoruso, G. Ausanio, A. C. Barone, R. Bruzzese, C. Campana, X. Wang, Appl. Sur. Sci. **254**, 1012 (2007).

[17] S. Amoruso, G. Ausanio, C. d. Lisio, V. Iannotti, M. Vitiello, X. Wang, L. Lanotte, Appl. Sur. Sci. **247,** 71 (2005).

[18] Q. Ou, T. Tanaka, M. Mesko, A. Ogino, M. Nagatsu, Diamond Relat. Mater. **17**, 664 (2008).

[19] J. Zhang, C. Q. Lan, Mater. Lett. **62,** 1521 (2008).

[20] A. V. Simakin, V. V. Voronov, N. A. Kirichenko, G. A. Shafeev, Appl. Phys. A **79**, 1127 (2004).

[21] F. Mafuné, J. Kohno, Y. Takeda, T. Kondow, J. Phys. Chem. B **104,** 8333 (2000).

[22] N. Takada, T. Sasaki, K. Sasaki, Appl. Phys. A **93**, 833 (2008).

[23] H. Zeng, Z. Li, W. Cai, B. Cao, P. Liu, S. Yang, J. Phys. Chem. B **111,** 14311 (2007).

[24] Changhao, Y. Shimizu, M. Masuda, T. Sasaki, N. Koshizaki, Chem. Mater. **16,** 963 (2004).

[25] B. M. Hunter, J. D. Blakemore, M. Deimund, H. B. Gray, J. R. Winkler, A. M. Muller, J. Am. Chem. Soc. **136**, 13118 (2014).

[26] T. E. Itina, J. Phys. Chem. C **115**, 5044 (2011).

[27] D. Paeng, D. Lee, J. Yeo, J. H. Yoo, F. I. Allen, E. Kim, H. So, H. K. Park, A. M. Minor, C. P. Grigoropoulos, J. Phys. Chem. C **119**, 6363 (2015).

[28] D. Riabinina, J. Zhang, M. Chaker, J. Margot, D. Ma, Nanotechnol. **2012,** 297863 (2012).

[29] A. Essaidi, M. Chakif, B. Schöps, A. Aumman, S. Xiao, C. Esen, A. Ostendorf, J. Laser Micro/Nanoeng. **8,** 131 (2013).

[30] D. M. Arboleda, J. M. J. Santillan, L. J. M. Herrera, M. B. F. van Raap, P. M. Zelis, D. Muraca, D. C. Schinca, L. B. Scaffardi, J. Phys. Chem. C **119**, 13184 (2015).

[31] J. D. Blakemore, H. B. Gray, J. R. Winkler, A. M. Muller, ACS Catal. **3**, 2497 (2013).

[32] M. Y. Sun, J. Yang, T. Lin, X. W. Du, RSC Adv. **2,** 7824 (2012).

[33] S. Machmudah, Wahyudiono, N. Takada, H. Kanda, K. Sasaki, M. Goto, Nanosci. Nanotechnol. **4,** 045011 (2013).

[34] A. Hamad, L. Li, Z. Liu, Appl. Phys. A **120**, 1247 (2015).

[35] Q. Cui, Y. Sha, J. Chen, Z. Gu, J. Nanopart. Res. **13**, 4785 (2011).

[36] H. X. Wang, X. Chen, J. Phys. D: Appl. Phys. **36**, 628 (2003).

[37] G. Yang, Laser Ablation in Liquids: Principles and Applications in the Preparation of Nanomaterials (CRC Press, Taylor & Francis Group, Boca Raton, FL, 2012), pp. 311.

[38] K.Y. Niu, J. Yang, S. A. Kulinich, J. Sun, H. Li, X. W. Du, J. Am. Chem. Soc. **132**, 9814 (2010).

[39] H. Y. Kwong, M. H. Wong, C. W. Leung, Y. W. Wong, K. H. Wong, J. Appl. Phys. **108,** 034304 (2010).

[40] A. H. Lu, W. C. Li, N. Matoussevitch, B. Spliethoff, H. Bönnemann, F. Schüth, Chem. Commun. **99,** 98 (2005).

[41] Y. L. Hsin, C. F. Lin, Y. C. Liang, K. C. Hwang, J. C. Horng, J. A. Ho, C. C. Lin, J. R. Hwu, Adv. Func. Mater. **18,** 2048 (2008).

[42] A. V. Simakin, V. V. Voronov, G. A. Shafeev, R. Brayner, F. B. –Verduraz, Chem. Phys. Lett. **348,** 182 (2001).

[43] N. Takada, T. Nakano, K. Sasaki, Appl. Phys. A **101,** 255 (2010).

[44] N. Luo, X. J. Li, X. H. Wang, F. Mo, H. T. Wang, Combust. Explo. Shock+, **46**, 609 (2010).

[45] Y. R. Uhm, C. K. Rhee, J. Nanomaterials, ID **427489** (2013) http://dx.doi.org/10.1155/2013/427489

[46] J. Li, Y. Wang, J. Tang, Y. Wang, T. Wang, L. Zhang, G. Zheng, J. Mater. Chem. A **3**, 2876 (2015)

[CHAPTER 3]

Formation of Au–Carbon Nanoparticles by Laser Ablation under Pressurized CO_2

Abstract

Pulsed laser ablation (PLA) is known to be a promising method for synthesizing metal nanoparticles. Here, Au–carbon nanoparticles were synthesized by PLA under pressurized carbon dioxide (CO_2). Au plate was ablated using a Nd: YAG laser with a wavelength of 532 nm and energy of 0.83 mJ in a high-pressure chamber. The experiments were performed at temperatures and pressures of 21-25°C and 7-15 MPa, corresponding to CO_2 densities of 0.75-0.89 g/cm^3, respectively. The synthesized products were collected on a silicon wafer and analyzed using field emission scanning electron microscopy (FE-SEM), transmission electron microscopy (TEM) and a scanning transmission electron microscopy (STEM) system equipped with energy dispersive X-ray spectroscopy (EDS). The results showed that the generated metal nanoparticles exhibited spherical and nanocluster structures. Au, C, and O were clearly found on the nanoparticle products.

Keywords: Gold nanoparticles; Gold–carbon particles; Pressurized CO_2; Laser ablation

3-1 Introduction

Bare metal nanoparticles easily oxidize and degrade under ambient conditions, and thus, many researchers have attempted to develop ways to prevent these issues. Synthesizing metal–carbon (i.e., carbon-coated) particles is recognized as an excellent way to enhance the chemical stability of the inner metals from oxidation and to improve their stability in harsh environments, such as acidic or basic environments and high

operating temperatures and/or pressures [1-3]. Moreover, metal–carbon nanoparticles may prevent the cores from agglomerating, and their biocompatibility enables using them for biomedical applications. In mechanical and electrochemical applications, metal–carbon nanoparticles may also exhibit improved thermal stability, wear resistance, and electrical conductivity [4].

Various techniques have been reported for synthesizing metal–carbon nanoparticles, such as arc discharge plasma, chemical vapor deposition (CVD), spray pyrolysis, and pulsed laser ablation (PLA). The simplest and most popular technique is the arc discharge plasma technique [5]. In this technique, two electrodes (carbon and metal electrodes) facing each other are connected to an electric power source to produce high-temperature plasma. The metal electrode enables producing the desired metal nanoparticles due to the high temperature of the plasma. The interaction between these metal nanoparticles with the carbon generated from the carbon electrode results in the formation of metal–carbon nanoparticles. Another simple technique is CVD, which may be easier to scale up for economically viable production. The process is conducted at temperatures of 600-1000°C and pressures of 40-100 Pa [6]. Similar to CVD, the spray pyrolysis technique is also performed at high temperatures (600-1000°C) [7,8]. The synthesized metal–carbon nanoparticles are produced by atomizing the reaction solution using a spray nozzle. This technique enables utilizing different types of precursors in the gas or liquid phase. In the PLA technique, a highly energetic laser beam interacts with a metal to disintegrate and vaporize the metal, forming a gaseous plasma containing atoms, molecules, ions, excited species, clusters, nanodroplets of melted material, etc., called the ablation plume. For metal–carbon nanoparticles, the metal target is generally immersed in a liquid medium. The metal–carbon nanoparticles can be

synthesized due to the interactions between metal nanoparticles and the carbon in the reaction medium, which quickly quenches the laser ablation plume [9,10].

In this paper, metal–carbon nanoparticles were synthesized using the PLA technique under pressurized carbon dioxide (CO_2). Au plates were used as the source metal for the nanoparticles. As an abundant natural carbon source, CO_2 is relatively benign with regard to both environmental and health effects. CO_2 has also found widespread application in a variety of industries because it is relatively non-reactive, non-toxic, nonflammable, and readily attainable critical properties. Moreover, the density of pressurized CO_2 can be adjusted by tuning the pressure and temperature [11,12]. As a result, the heat and mass transfer rates of pressurized CO_2 are considerably higher than those of CO_2 at ambient condition, which is beneficial for generating metal–carbon nanoparticles by the PLA technique. Furthermore, employing CO_2 as the reaction medium has been shown to prevent contaminating the generated nanoparticles with impurities from the organic solvents usually used as a reaction medium [9,10]. This paper presents further insight from the previously reported gold nanoparticles synthesis via PLA in pressurized or supercritical CO_2 [11,13,14] since we conducted more comprehensive analysis. We demonstrate that the generated Au nanoparticles were not pristine Au nanoparticles as believed in earlier studies, but the composite of Au and C nanoparticles.

3-2 Materials and Methods

Figure 1 shows a schematic diagram of the laser ablation system used to generate nanoparticles under pressurized CO_2. Au plate, purchased from Nilaco Co., Japan, with dimensions of 10 × 10 mm and a thickness of 1 mm was used as the target

material. A silicon wafer with a thickness of 1 mm and dimensions of 7 × 7 mm, also purchased from Nilaco Co, Japan, was employed as the collector for the generated particles. CO_2 (99.95%) was supplied from Sogo Co., Japan and used as the reaction medium.

A high-power Q-switched pulsed Nd: YAG laser (Spectra-Physics Quanta-Ray INDI-40-10), with a wavelength of 532 nm, pulse energy of 0.83 mJ, pulse rate of 10 Hz, and pulse duration of approximately 8 ns, was used to ablate the metal target, which was placed at the center of a high-pressure chamber constructed from SUS 316 stainless steel (110 mL in volume, 6.5 cm in diameter, AKICO, Japan), and the Nd:YAG laser was located approximately 1 m from the target. The laser beam was focalized by a 1-mm-diameter of apperture. The silicon wafer was placed beneath the Au target in order to collect the generated nanoparticles. Figure 1 also shows the positions of the metal plate and Si wafer inside high-pressure chamber. CO_2 was pressurized and pumped into the chamber using a high-performance liquid chromatography (HPLC) pump (PU-1586, Jasco Co., Japan). The chamber temperature was regulated with a temperature controller, and the pressure was controlled with a back-pressure regulator. The temperature and pressure ranges for the experiments were 21-25°C and 7-15 MPa corresponding to 0.75-0.89 g/cm^3 of CO_2 density, respectively. A thermocouple for monitoring the experimental temperature was inserted into the chamber. K-type thermocouples were also inserted into the chamber's walls to measure the radial temperature distribution. After the desired pressure and temperature were attained, PLA was performed for 15 min. After the CO_2 medium naturally evaporated, the particles deposited on the silicon wafer were collected and then characterized by field emission scanning electron microscopy (FE-SEM, Model JSM-6330F, JEOL, Japan). Particle

size characterization was also performed using (scanning) transmission electron microscopy, (S)TEM, with a JEM-2100F HK model operating at 200 kV and equipped with CCD camera. (S)TEM samples were prepared by placing carbon grids below the target material in the same position as that of the Si wafer to collect the particles. In order to determine the products elemental composition, scanning transmission electron microscopy with energy dispersive X-ray spectroscopy (STEM-EDS) (Model JEM-2100F HK, JEOL, Japan) was also performed.

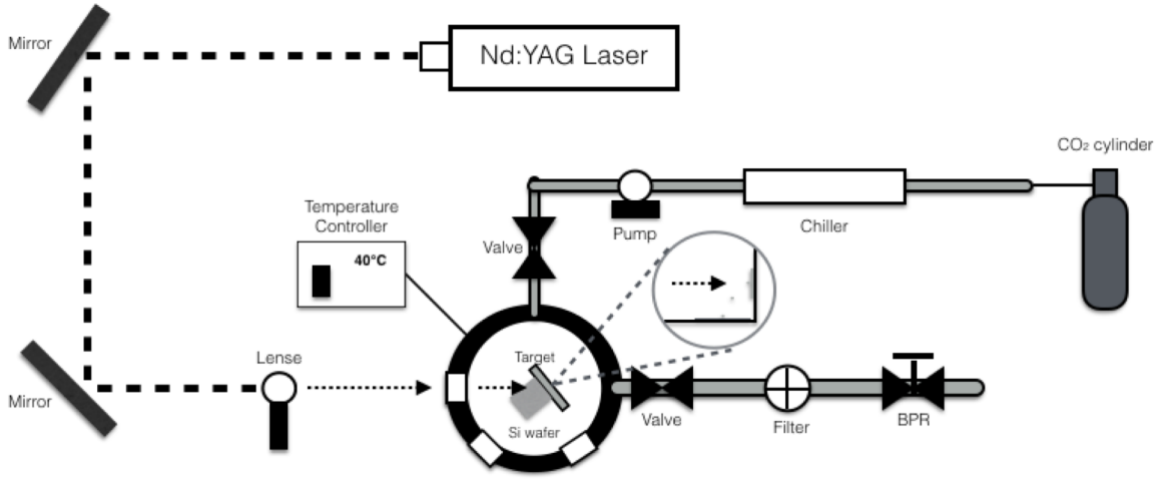

Figure 1. Schematic diagram of PLA under pressurized CO_2.

3-3 Results and Discussion

In previous studies, when CO_2 was employed as the medium for generating metal–carbon nanoparticles, one of the important advantages that PLA in CO_2 exhibited over the conventional multistep chemical synthesis techniques was the absence of contaminants, which may come from the intermediate medium. Applying PLA directly to the metal target eliminates the need for chemical precursors and enables generating clean nanoparticles. Figure 2 shows FE-SEM and scanning TEM (STEM) images of Au nanoparticles generated by PLA under pressurized CO_2 with a density 0.75 g/cm^3.

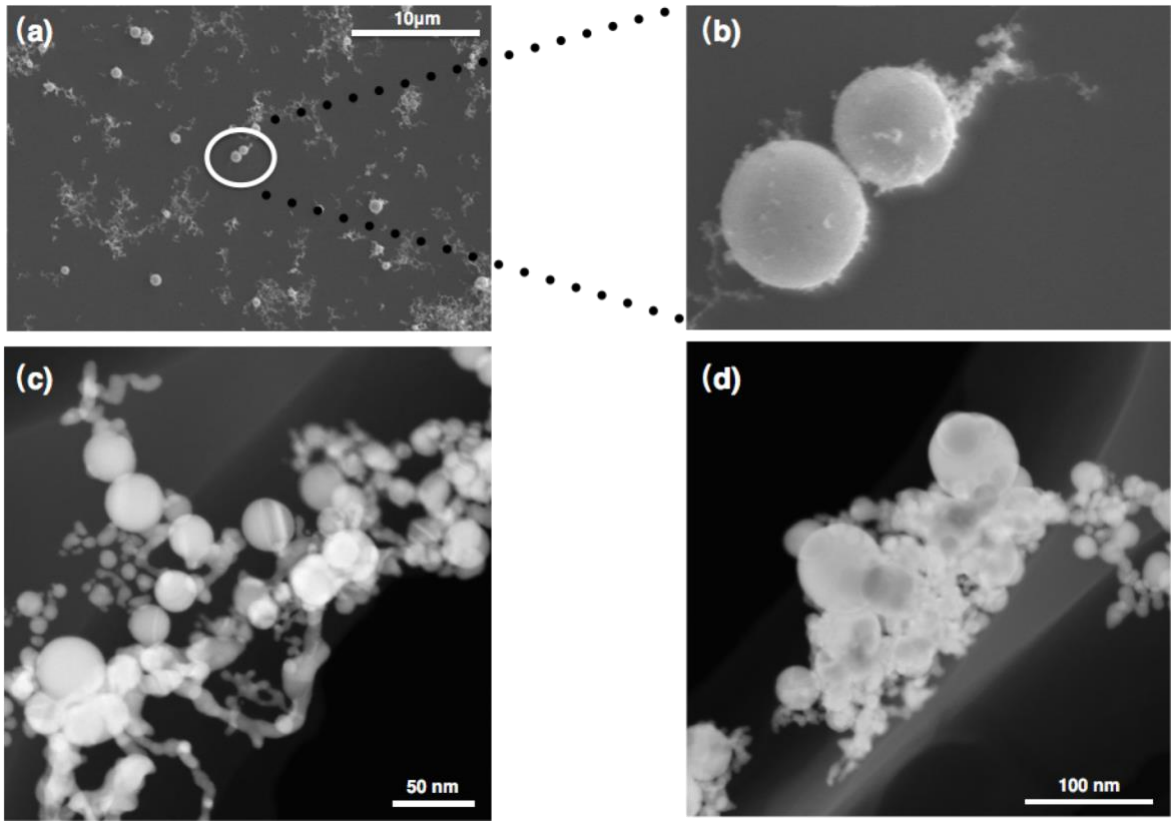

Figure 2. (a), (b) FE-SEM and (c), (d) STEM images of Au nanoparticles generated by PLA at density 0.75 g/cm^3 (7.3 MPa; 23.4°C).

As discussed above, plasma, vapor, and nano/micro-sized molten metallic droplets could be generated as initial products when the pulsed laser beam was introduced to heat the metal target. These products then reacted with elements in the reaction medium to produce nanoparticles [9,10]. Consequently, the generated metal nanoparticles consisted of spherical and nanocluster structures. Employing highly compressed CO_2 as the medium enabled achieving large changes in density with small changes in temperature and/or pressure. Thus, pressurized CO_2 may lead to the formation of a colloidal medium. As a result, the generated Au nanoparticles were also mainly composed of spherical and nanocluster structures, as shown in Fig. 2. In the images, a network structure of smaller Au nanoclusters seems to surround larger Au nanoparticles.

This arrangement may form due to the fast coagulation and quenching of the Au atoms in the dense CO_2 environment [13]. Saitow et al. [14] performed nanosecond PLA with an excitation wavelength of 532 nm in supercritical CO_2 to produce Au nanoparticles. Those Au nanoparticles exhibited two different morphologies: large nanospheres and nanonecklaces (nanoclusters). They reported that the nanonecklaces were a few tens of micrometers long, and the large Au nanospheres were 500 nm in diameter. Similar results were also reported by Machmudah et al. [13]. They performed PLA under pressurized CO_2 at pressures of 0.2-20 MPa and temperatures of 20-80°C, which generated spherical Au nanoparticles and a network structure of small Au nanoparticles.

When CO_2 is pressurized and heated above its critical point, CO_2 exhibits interesting properties such as a liquid-like density and gas-like viscosity, and the diffusion coefficients in these conditions are higher than those of liquids. When the temperature of CO_2 is lower than its critical temperature and more pressure is applied, CO_2 becomes denser. At these conditions, CO_2 may have liquid-like properties, but no liquid forms. Similar to supercritical CO_2, the advantages of dense CO_2 as a reaction medium over other solvents are primarily due to its physicochemical properties. Dense CO_2 is an intermediate between a gas and a liquid, and its properties are easily adjustable by shifting the temperature and pressure [15]. Therefore, when PLA was applied in dense CO_2 as the medium, high-density plasmas were also generated [9]. Figure 3 shows FE-SEM and STEM images of Au nanoparticles generated by PLA under pressurized CO_2 with various CO_2 densities.

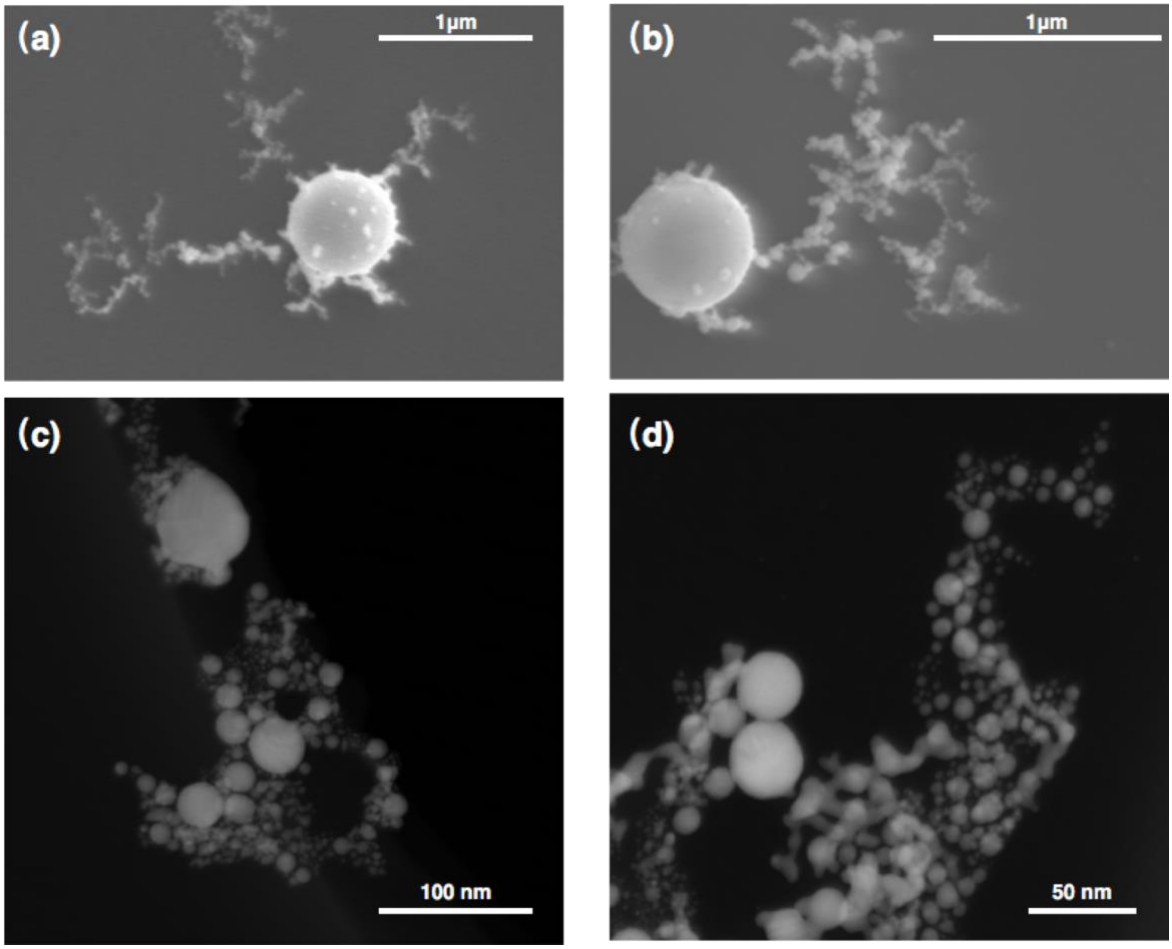

Figure 3. FE-SEM (top) and STEM images (bottom) of Au nanoparticles generated by PLA at CO_2 densities of (a), (c) 0.80 g/cm^3 (9.1 MPa; 24.5°C) and (b), (d) 0.89 g/cm^3 (17.5 MPa; 25.1°C)

It should be noted that no experiments were conducted with low-density CO_2 (less than 0.60 g/cm^3) in order to maintain liquid-like physical properties, which require densities of around 0.60-1.6 g/cm^3. The generated Au nanoparticles clearly exhibited nanosphere-like and nanocluster morphologies. Nanoparticles formed when the PLA was applied at CO_2 densities of 0.75 (Fig. 2) and 0.80 g/cm^3 (Fig. 3). As the CO_2 density increased (0.89 g/cm^3), the generated Au nanoparticles were also apparently composed of Au nanoclusters and the Au nanosphere-like structure. The Au nanosphere-like structure generated at 0.89 g/cm^3 in Fig. 3 appears smaller than those

generated under other conditions. Similar to the generation of metal nanoparticles by PLA in aqueous media, the production of Au nanoparticles by PLA under high-density CO_2 was affected by several parameters such as laser fluence, irradiation time, excitation wavelength, pulse width, and the CO_2 phase [9,14,16]. Generally, the PLA plasma plume evolution in a confining liquid leads to cluster formation, nucleation, and crystals growth during the ablation process. Hence, the PLA plasma plume in high-density CO_2 will also rapidly quench in the confining liquid-like CO_2. As a result, the short quenching times of the PLA plasma plume enables restricting the size of the grown Au particles and producing Au nanoclusters [9]. Saitow et al. [14] performed PLA in supercritical CO_2. They showed that nanoparticles and nanoclusters could be produced and deposited since these products were not soluble in supercritical CO_2. They reported that the size of the generated nanosphere particles did not depend on the density of the CO_2 medium.

In addition, we measured the particle size distribution of the generated particles using the ImageJ program to analyze TEM images. Figure 4 shows typical TEM micrographs of generated Au particles in pressurized CO_2. Similar to the SEM images, the TEM images in Fig. 4(a), (b) and (c) indicate that the particles generated under each set of conditions are spherical. These results are similar to those of a work previously reported on PLA in liquid CO_2 using a Nd: YAG laser with a laser energy of 2.46 mJ [16].

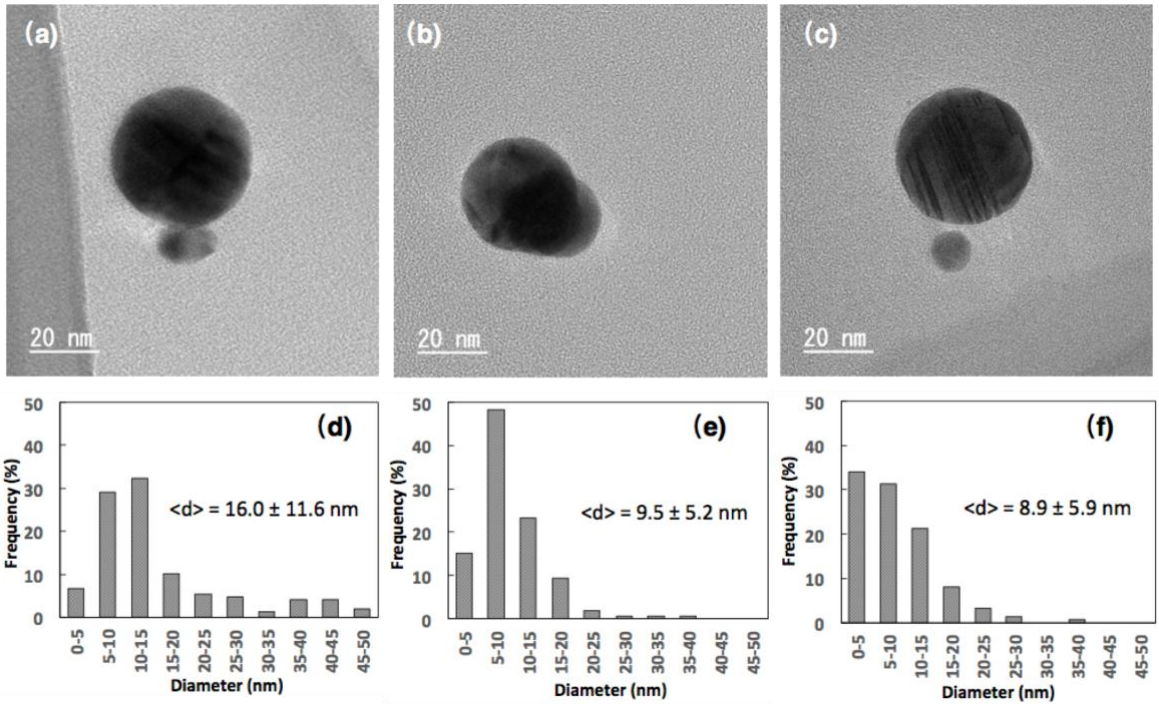

Figure 4. TEM images (top) and size distributions (bottom) of Au nanoparticles generated by PLA at CO_2 densities of (a), (d) 0.75 g/cm^3 (7.3 MPa; 23.4°C), (b), (e) 0.80 g/cm^3 (9.1 MPa; 24.5°C), and (c), (f) 0.89 g/cm^3 (17.5 MPa; 25.1°C).

Au nanoparticles prepared by PLA in pressurized CO_2 were well dispersed and exhibited a broad size distribution, as shown in Fig. 4. At an identical laser power of 0.83 mJ, the average size of nanoparticles decreased from 16.0 to 8.9 nm with the density of CO_2 increasing from 0.75 to 0.89 g/cm^3. We note that some literatures report that nanoparticles synthesized in the pressurized liquid medium via PLA has smaller size with increasing medium pressure (or increasing density). For instance, the average size of ZnO nanoparticles synthesized in water [24,25] decreased from 50 - 100 nm at ambient condition down to below 20 nm at 31 MPa at constant temperature. Sn nanoparticles synthesized in pressurized CO_2 exhibits similar phenomenon [26]. Thus, it

can be safely generalized that increasing the pressure of the medium has the effect to decrease the size of nanoparticles.

STEM-EDS was performed to analyze the presence of carbon on the generated nanoparticles. Several reports [9,16,21,22,23] have concluded that the PLA reaction medium and ablated matter can react during the formation of particles. However, the alloy nanoparticle formation mechanism during PLA and the process mechanisms are still not well understood. Figure 5 shows the STEM-EDS mapping of nanoparticles generated in CO_2 with various densities.

In order to understand the chemical composition of the generated Au nanoparticles, they were characterized using a STEM system equipped with EDS. This method distinguishes the characteristic X-rays emitted from the analyte by their energy levels. Since each element has a unique atomic structure, the atomic structure could be identified individually from one another. Hence, EDS analysis is a reliable way to investigate the sample using the interactions between electromagnetic radiation and matter.

Figure 5 shows STEM images and EDS patterns of the generated Au nanoparticles when PLA was applied at CO_2 densities of 0.70, 0.80 and 0.89 g/cm^3. The EDS spectrum clearly shows that the Au, C, and O were detected.

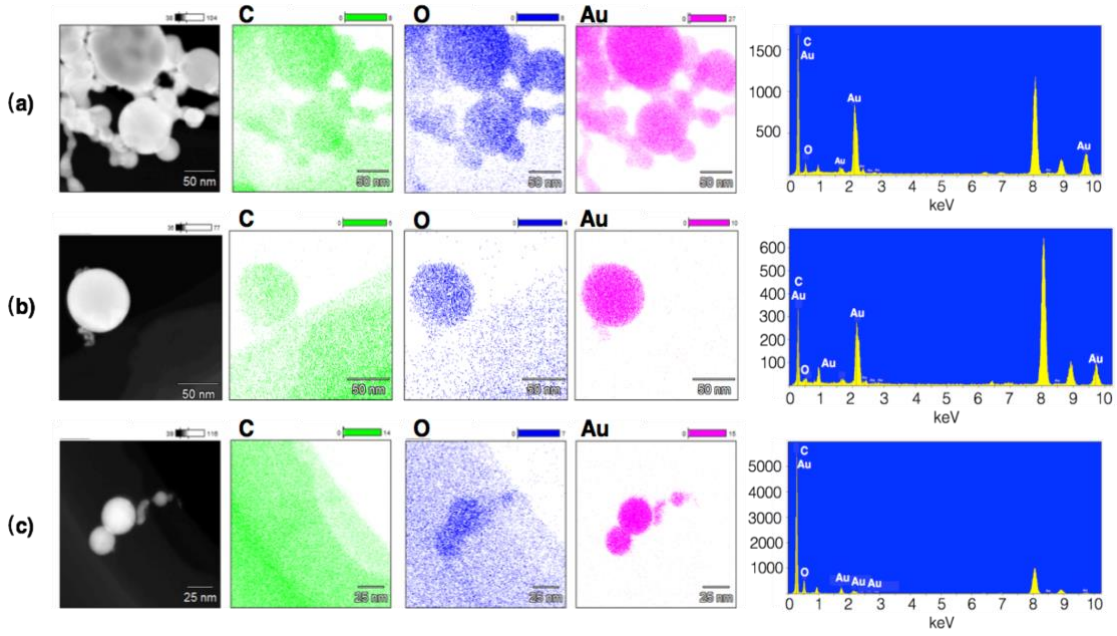

Figure 5. EDS mappings of particles generated at CO_2 densities of (a) 0.75 g/cm^3, (b) 0.80 g/cm^3, and (c) 0.89 g/cm^3.

The spectroscopic analysis demonstrated that the generated particles were almost completely composed of Au under each set of conditions. The spectra clearly exhibit a high C peak due to the TEM grid, which contains considerable C. O was also detected by spectroscopy, although the peak was not high compared to those of Au and C. However, particles generated under all conditions contained Au, C and O. As a reaction medium, CO_2 is well known to decompose into C and O during PLA [19,20], as evidenced in Fig. 5. Interestingly, Au, C, and O were uniformly distributed on the outermost surface, which could be attributed to the dissociation of the CO_2 reaction medium into CO molecules, C atoms, and O atoms during PLA. The CO_2 dissociation products may induce chain reaction with other CO_2 molecules. The possible phenomenon that occurred is the reactive C, CO and O collide with other CO_2 molecules or themselves to form a large hollow carbon nanostructure layer (i.e. “sp2

amorphous carbon") that covers the Au nanoparticles and nanoclusters [19]. The O atoms can oxidize the carbon nanostructure since O can still be covalently bound to the sp2 amorphous carbon type nanostructure. However, the EDS spectra indicate that there is only a trace amount of O on the nanostructures, indicating that only partial oxidation occurred. Therefore, C and O were both observed on the generated Au nanoclusters in this study.

Further, the corresponding selected area diffraction pattern of generated particles in each condition are shown in Fig. 6. The characteristic rings in polycrystalline diffraction pattern can be indexed to the {111}, {200}, {220}, and {311} planes for each condition, that expected from fcc Au. These results are witnessed our previous explanation, that almost particles are formed by gold and only partial part of generated particles are formed by carbon.

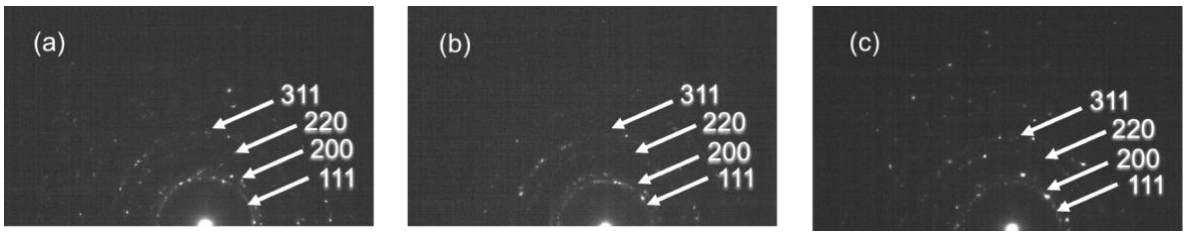

Figure 6. Electron diffraction pattern of particles generated at CO_2 densities of (a) 0.75 g/cm^3, (b) 0.80 g/cm^3, and (c) 0.89 g/cm^3.

3-4 Conclusion

Au nanoparticles with carbon were successfully synthesized using the PLA method under pressurized CO_2. The PLA was carried out at temperatures of 21-25°C with CO_2 densities of 0.75-0.89 g/cm^3 and an irradiation time 15 min. The generated nanoparticles were characterized using a STEM system equipped with EDS. SEM images exhibited generated metal nanoparticles with spherical and nanocluster

morphologies. The network structure of smaller metal nanoclusters appears to surround the larger metal nanoparticles. Au, C, and O were found to be uniformly distributed on the generated nanoclusters. The results suggest that this method enables obtaining advanced nanostructured materials.

3-5 References

[1] Wang, S., Huang, X., He, Y. et al. (2012). Synthesis, Growth Mechanism and Thermal Stability of Copper Nanoparticles Encapsulated by Multi-layer Graphene. *Carbon*, 50: 2119-2125.

[2] Love, C.A., Cook, R.B., Harvey, T.J., Dearnley, P.A., Wood, R.J.K. (2013). Diamond Like Carbon Coatings for Potential Application in Biological Implants—A Review, *Tribology International*, 63: 141-150.

[3] Espinoza-Rivas, A.M., Pérez-Guzmán, M.A., Ortega-Amaya, R., Santoyo-Salazar, J., Gutiérrez-Lazos, C.D., Ortega-López, M. (2016). Synthesis and Magnetic Characterization of Graphite-Coated Iron Nanoparticles, *Journal of Nanotechnology*, 2016: 6.

[4] Sattler, Klaus D. ed. (2010). *Handbook of Nanophysics: Principles and Methods*, CRC Press, Taylor and Francis Group, LLC.

[5] Wei, Z.Q., Liu, L.G., Yang, H. et al. (2011). Characterization of Carbon Encapsulated Fe-nanoparticles Prepared by Confined Arc Plasma, *Transactions of Nonferrous Metal Society of China*. 21: 2026-2030.

[6] Sarno, M., Cirillo, C., Ciambelli, P. (2014). Selective Graphene Covering of Monodispersed Magnetic Nanoparticles, *Chemical Engineering Journal*. 246: 27-38.

[7] Jung, D.S., Park, S.B., Kang, Y.C. (2010). Design of Particles by Spray Pyrolysis and Recent Progress in its Application, *Korean Journal of Chemical Engineering*. 27: 1621-1645.

[8] Atkinson, J.D., Fortunato, M.E., Dastgheib, S.A. et al. (2011). Synthesis and Characterization of Iron-impregnated Porous Carbon Spheres Prepared by Ultrasonic Spray Pyrolysis. *Carbon*. 49: 587-598.

[9] Yang, G.W. (2007). Laser Ablation in Liquids: Applications in the Synthesis of Nanocrystals. *Progress in Materials Science*. 52: 648-698.

[10] Zeng, H., Du, X.W., Singh, S.C. et al. (2012). Nanomaterials via Laser Ablation/Irradiation in Liquid: A Review. *Advanced Functional Materials*. 22: 1333-1353.

[11] Machmudah, S., Wahyudiono, Kuwahara, T., Sasaki, M., Goto, M. (2011). Nano-structured Particles Production Using Pulsed Laser Ablation of Gold Plate in Supercritical CO_2. *Journal of Supercritical Fluids*. 60: 63-68.

[12] Machmudah, S., Sato, T., Wahyudiono, Sasaki, M., Goto, M. (2012). Silver Nanoparticles Generated by Pulsed Laser Ablation in Supercritical CO_2 Medium. *High Pressure Research*, 32: 60-66.

[13] Machmudah, S., Wahyudiono, Takada, N., Kanda H., Sasaki, K., Goto, M. (2013). Fabrication of Gold and Silver Nanoparticles with Pulsed Laser Ablation Under Pressurized CO_2, *Advances in Natural Sciences: Nanosciences and Nanotechnology*. 4: 045011-045018.

[14] Saitow, K., Yamamura, T., Minami T. (2008). Gold Nanospheres and Nanonecklaces Generated by Laser Ablation in Supercritical Fluid. *Journal of Physical Chemistry C*. 112: 18340-18349.

[15] Sanli, D., Bozbag, S.E., Erkey, C. (2012). Synthesis of Nanostructured Materials Using Supercritical CO_2: Part I. Physical Transformations. *Journal of Materials Science*. 47: 2995-3025.

[16] Mardis, M., Takada, N., Machmudah, S., Wahyudiono, Sasaki, K., Kanda H., Goto, M. (2016). Nickel Nanoparticles Generated by Pulsed Laser Ablation in Liquid CO_2. *Research on Chemical Intermediates*. 42: 4581-4590.

[17] Boutinguiza, M., Comesaña, R., Lusquiños, F., et al. (2015). Production of Silver Nanoparticles by Laser Ablation in Open Air. *Applied Surface Science*. 336: 108-111.

[18] Minaev, N.V., Arakcheev, V.G., Rybaltovskii, A.O., et al. (2015). Dynamics of Formation and Decay of Supercritical Fluid Silver Colloid under Pulse Laser Ablation Conditions. *Russian Journal of Physical Chemistry B*. 9: 1074-1081.

[19] Fukuda, T., Maekawa, T., Hasumura, T., et al. (2007). Dissociation of Carbon Dioxide and Creation of Carbon Particles and Films at Room Temperature. *New Journal of Physics*. 9: 321.

[20] Nakahara, S., Stauss, S., Kato, T. et al. (2011). Synthesis of Higher Diamondoids by Pulsed Laser Ablation Plasmas in Supercritical CO_2. *Journal of Applied Physics*. 109: 123304.

[21] Moslehirad, F., Majles Ara, M.H., Torkamany, M.J. (2013). Synthesis of composite Au/TiO_2 nanoparticles through pulsed laser ablation and study of their optical properties. *Laser Physics*. 23: 075601.

[22] Amendola, V., Scaramuzza, S., Carraro, F. et al. (2016). Formation of alloy nanoparticles by laser ablation of Au/Fe multilayer films in liquid environment. *Journal of Colloid and Interface Science*. 489: 18-27.

[23] Hajiesmaeilbaigi, F., Motamedi, A., Ruzbehni, M. (2009). Synthesis and Characterization of Composite Au/TiO_2 Nanoparticles by Laser Irradiation. *Laser Physics*. 20: 508-511.

[24] S. Kulinich, T. Kondo, T. Shimizu et al. (2013) Pressure effect on ZnO nanoparticles prepared via laser ablation in water. *Journal of Applied Physics*. 113: 033509.

[25] W. Soliman, N. Takada, N. Koshizaki et al. (2013). Structure and size control of ZnO nanoparticles by applying high pressure to ambient liquid in liquid-phase laser ablation. *Applied Physics A*. 10: 779

[26] M. Koizumi, S. Kulinich, Y. Shimizu et al. (2013). Medium slow dynamics of ablated zone observed around the density fluctuation ridge of fluid medium. *Journal of Applied Physics*. 114: 214301.

[CHAPTER 4]

Consideration of Au–Carbon Nanoparticles by Laser Ablation under Supercritical CO_2

Abstract

In our previous works, we observed the formation of Au-carbon nanoparticles via pulsed laser ablation (PLA) under pressurized CO_2. We showed that the size of the generated nanoparticles depend strongly on the pressure and the temperature of the CO_2 medium. Here, we further elaborate this finding by applying more extreme conditions for the CO_2 medium. The experiments were performed at temperatures and pressures of 31-80 °C and 5-15 MPa, corresponding to the supercritical phase of CO_2. We observed that the generated Au-carbon nanoparticles has the average size of 11 nm with spherical and nanocluster structures. The effects of the medium temperature and pressure will be discussed thoroughly.

4-1 Introduction

Gold nanoparticles show promising technological applications in the field of chemistry, physics and biology. For instance, the unique chemical properties of gold nanoparticles, which are believed due to the relativistic effects, enable their application as catalysts [1] where depending on the size, larger gold particles show less catalytic activity compared to the smaller gold nanoparticles. For such a metal, bulk gold is usually considered as inactive catalyst. One of the remarkable properties of gold nanoparticles is their optical property due to localized surface plasmon resonance

(LSPR). The main application of LSPR in gold nanoparticles is in the field of biophysics where they can be used as biomolecule sensors, bio-imaging for cancer treatment and photothermal cancer therapy [2]. Therefore, an efficient way to synthesize gold nanoparticles is one of the main issues to efficiently utilize the gold nanoparticles for the aforementioned technological applications.

The simplest technique to synthesize gold nanoparticles is probably an arc discharge plasma technique [3]. In this technique, as an example, two titanium electrodes in HAuCl4 solution are connected to an electric power source to produce high-temperature plasma. The HAuCl4 is directly reduced into Au due to the electron transfer from the plasma zones. The electrode enables producing the desired metal nanoparticles due to the high temperature of the plasma.

Pulse laser ablation (PLA) in liquid or compressed fluid is one of the alternative methods to synthesize nanoparticles. This method has been considered as a clean, facile and rapid way to synthesize the nanoparticles since it requires minimal amount of chemicals and also gives less byproducts and residues. Since laser has the strong ability to ablate many types of material, it can be used to produce almost any inorganic type nanomaterials including metals, oxides, sulfides and among others. New phases of nanomaterials can be attained using this method where the other conventional methods usually fail [4].

Recently, there have been plenty of reports on the laser ablation method to produce Au nanoparticles from Au plate immersed in pure liquid media such as water [5–10], n-decane [11], dimethylsulfoxide (DMSO), tetrahydrofuran (THF), acetonitrile (ACN) [12], chloroform [13], ethanol [13] and toluene [13,14]. The Au nanoparticles

generated in those media have the size of 1.8-18 nm, depending on the laser wavelength, duration and the fluence.

In the previous gold nanoparticles synthesis using PLA method, we discovered that the Au nanoparticles generated in liquid (pressurized) CO_2 are not pristine Au nanoparticles [15]. Instead, the Au nanoparticles are coated by the carbon nanostructures, which was generated due to the dissociation of the CO_2 molecules by the incoming photons. Hence, the new class of nanomaterials might be discovered as the side reaction due to the laser irradiation.

Motivated by these findings, we further elaborate this finding by applying more extreme conditions for the CO_2 medium. The experiments were performed at temperatures and pressures of 31-80 ℃ and 8-15 MPa, corresponding to the supercritical phase of CO2. We observed that the generated Au-carbon nanoparticles has the average size of 11 nm with spherical and nanocluster structures.

4-2 Experimental

4-2-1 Materials

Gold plates with each area of 10 × 10 mm and a thickness of 1 mm (99.95%; Nilaco Co., Japan) were prepared as the target material filled with CO_2 (99.95%; Sogo Co., Japan) as the PLA medium. A micro grid was purchased from Okenshoji Co., Ltd Japan, was employed as the collector for the generated particles.

4-2-2 Methods

The experimental setup to generate nanoparticles has been developed by our groups and described in our previous works [15–21]. Briefly, the instruments consist of a 110 mL with 6.5 cm diameter high-pressure chamber constructed from SUS 316 stainless steel,

a high-power Q-switched pulsed Nd:YAG laser (Spectra-Physics Quanta-Ray INDI-40-10), a lens with a aperture of a 1 mm hole and mirrors. CO_2 was pressurized and pumped into the chamber using a high-performance liquid chromatography (HPLC) pump (PU-1586, Jasco Co., Japan). The chamber temperature was regulated with a temperature controller, and the pressure was controlled with a backpressure regulator. The gold target was placed at the center of a high-pressure chamber, approximately 1 m from the laser and irradiated with the Nd:YAG laser operated with a wavelength of 532 nm, pulse energy of 0.83 mJ, a pulse rate of 10 Hz, and pulse duration of approximately 8 ns. The silicon wafer was placed beneath the Au target in order to collect the generated nanoparticles.

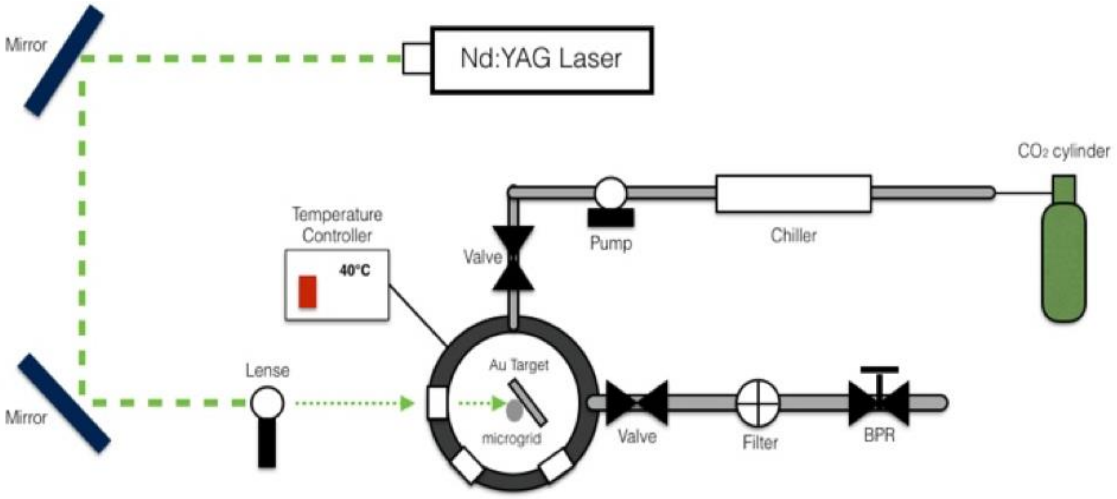

Figure 1. Experimental apparatus of PLA.

The temperature and pressure ranges for the experiments were 31-80 °C and 8-15 MPa corresponding to the supercritical phase of CO_2. A thermocouple for monitoring the experimental temperature was inserted into the chamber. K-type thermocouples were also inserted into the chamber's walls to measure the radial temperature distribution. After the desired pressure and temperature were attained, PLA was performed for 15 min. After the CO_2 medium naturally evaporated, the particles

deposited on the silicon wafer were collected and then characterized by field emission scanning electron microscopy (FE-SEM, Model JSM-6330F, JEOL, Japan).

Particle size characterization was also performed using (scanning) transmission electron microscopy, (S)TEM, with a JEM-2100F HK model operating at 200 kV and equipped with CCD camera. (S)TEM samples were prepared by placing carbon microgrid below the target material in the same position as that of the Si wafer to collect the particles. In order to examine the products elemental composition, scanning transmission electron microscopy with energy dispersive X-ray spectroscopy (STEM-EDS) (Model JEM-2100F HK, JEOL, Japan) was also performed.

4-3 Results and Discussion

4-3-1 Effect of Pressure

The effect of the pressure on the average size of the gold nanoparticle was examined at 40 °C. The TEM images and the particle size distribution are displayed in Fig. 2. The results show that increasing the pressure generally decrease the size of the gold nanoparticles [22]. Therefore, the smallest average nanoparticles were obtained at 12 MPa with 9.0 nm. Previous studies report that the average size of several nanoparticles synthesized in the pressurized liquid medium via PLA has smaller size with increasing medium pressure. Zirconia nanoparticles synthesized in water [22,23] decreased from 50 - 100 nm to below 20 nm at the ambient condition of 31 MPa and a constant temperature. Tin nanoparticles synthesized in pressurized CO_2 exhibits similar phenomenon [24]. We presume that similar effect applies also on the generated gold nanoparticles in supercritical CO_2.

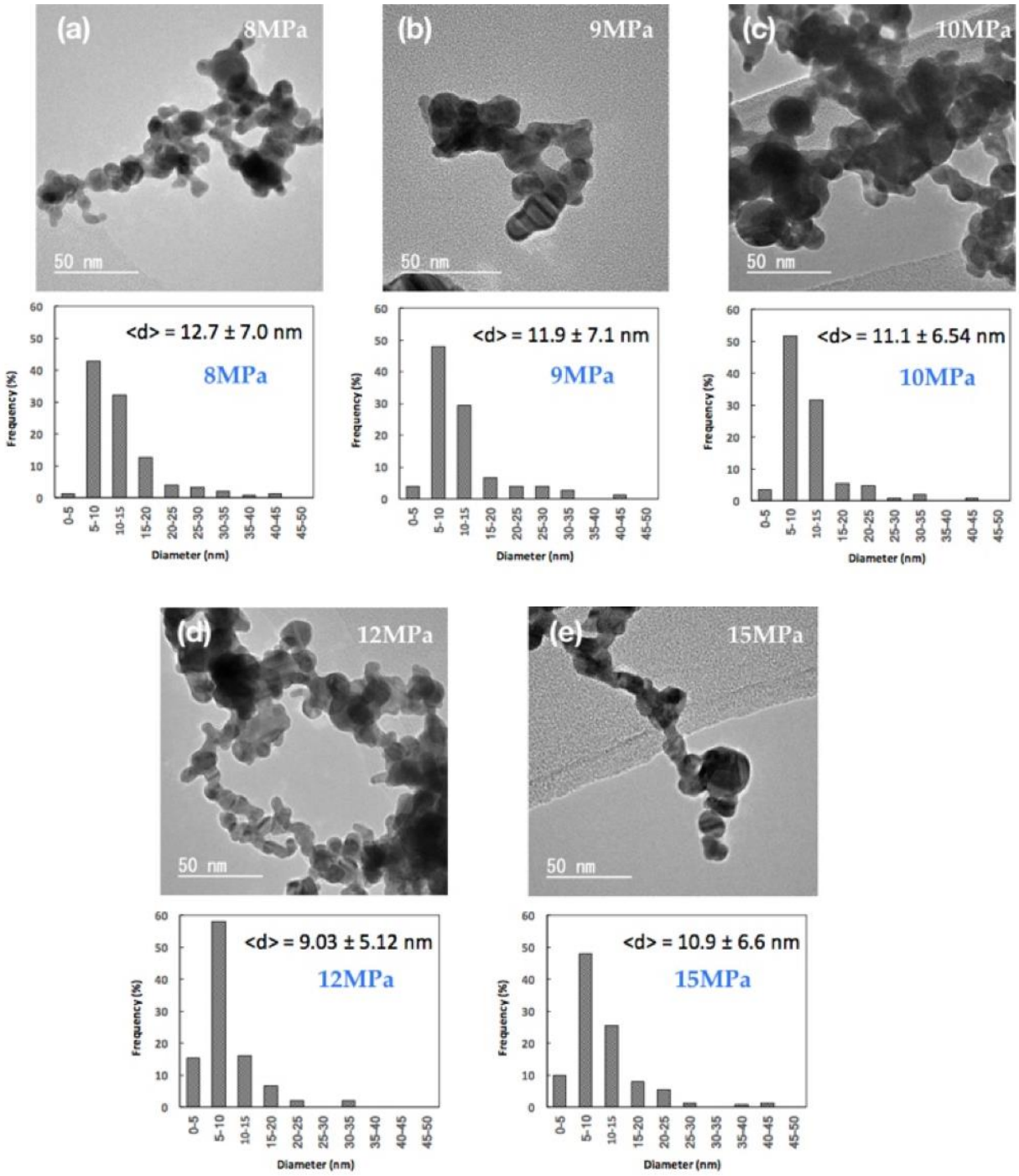

Figure 2. TEM images and size distirbution of generated Au particles at 40 ^{o}C with different pressures (a) 8 MPa; (b) 9 MPa; (c) 10 MPa; (d) 12 MPa; (e) 15 MPa.

4-3-2 Effect of Temperature

The effect of the temperature on the average size of the gold nanoparticle was determined at 8MPa. The TEM images and the particle size distribution are displayed in Fig. 3. The results show that increasing the temperature generally decrease the size of the gold nanoparticles with the smallest average nanoparticles were obtained at 60 °C with 11.0 nm.

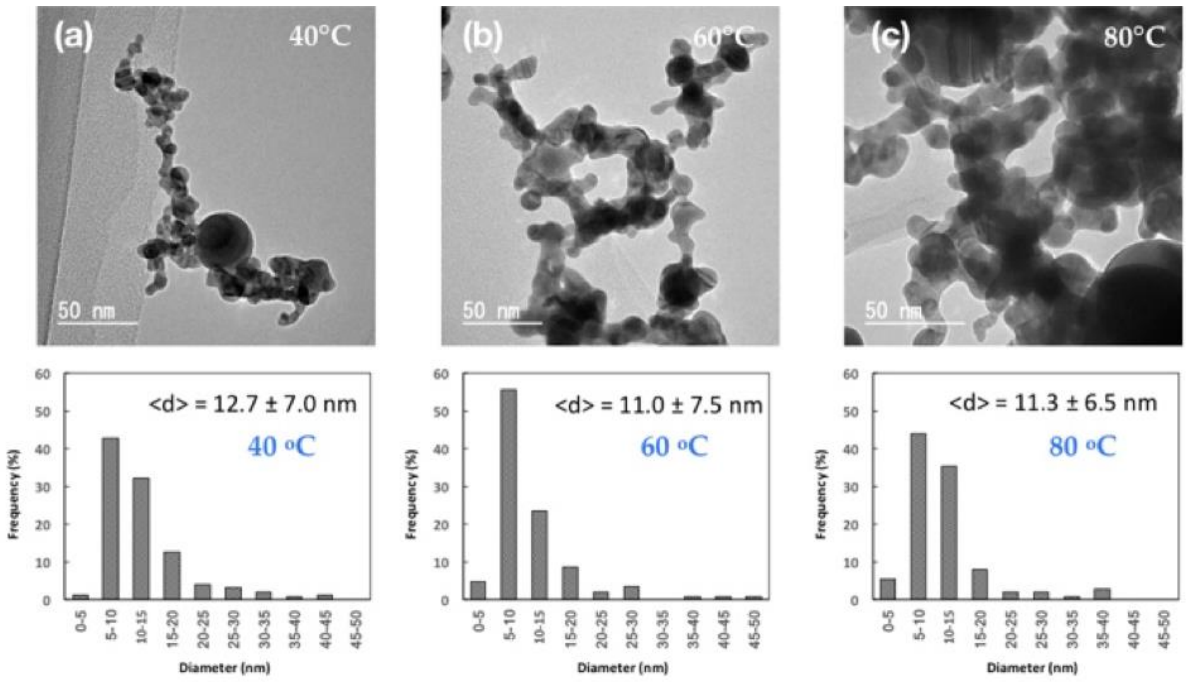

Figure 3. TEM images and size distirbution of generated Au particles at 8 MPa different temperatures (a) 40 °C; (b) 60 °C; (c) 80 °C.

As can be seen in the figure 2 and 3, in the supercritical phase of CO_2, increasing pressure at constant temperature will yield smaller nanoparticles with the minimum at 12 MPa. Similarly, increasing the temperature at constant pressure will yield smaller nanoparticles with the minimum at 60 °C. It can thus be extrapolated that the smallest Au nanoparticle will be generated under the condition of temperature and

pressure of 60 °C and 12 MPa, respectively. It can be expected that the average size of the Au nanoparticle is 7.6 nm under that condition.

Based on the results above, the generated nanoparticles are spherical in shape due to the nucleation occurred in the liquid and expand their size in the direction where the pressure stress is minimal [25]. In the case of liquid medium, all directions in the space are equal. Therefore, the nanoparticles can have spherical shape in the liquid medium.

4-3-3 Elemental Analysis

In order to understand the chemical composition of the generated Au nanoparticles, they were characterized using a STEM system equipped with EDS. This method distinguishes the characteristic X-rays emitted from the analyte by their energy levels. Since each element has a unique atomic structure, the atomic structure could be identified individually from one another. Hence, EDS analysis is a reliable way to investigate the sample using the interactions between electromagnetic radiation and matter.

Fig. 4 shows STEM images and EDS patterns of the generated Au nanoparticles sample when PLA was applied at CO_2 temperature of 40 °C and pressure of 10 MPa. The EDS spectrum clearly shows that the Au, C, and O were detected.

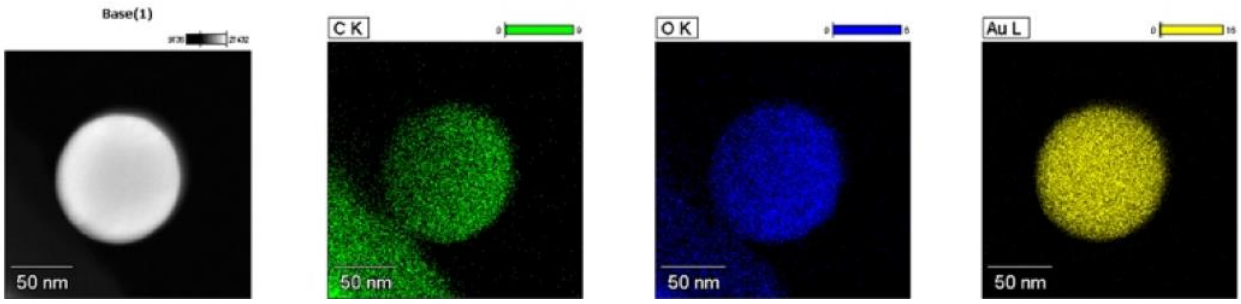

Figure 4. Energy-dispersive X-ray spectroscopy mappings of particles generated at 40°C and 10 MPa of supercritical CO_2.

No proper explanation for the exact mechanism of laser induced nanoparticles formation has been deduced due to the complexity of the process since the system is non-equlibrium [4]. However, the general physics behind nanomaterial creation via laser ablation can be simply viewed as the photon-electron, electron-electron and phonon-electron interactions [26]. In our experiment the Au nanoparticles were created from the pristine metal. The key point of the successful creation of the nanomaterial is the ability of the laser energy to eject some of the material from the bulk phases to the liquid medium phases in order to form the nanoparticles. Due to laser interaction with the bulk material more complex process may occur. The process includes heating, melting, ionization/vaporization and plasma plume creation as displayed in Fig. 5.

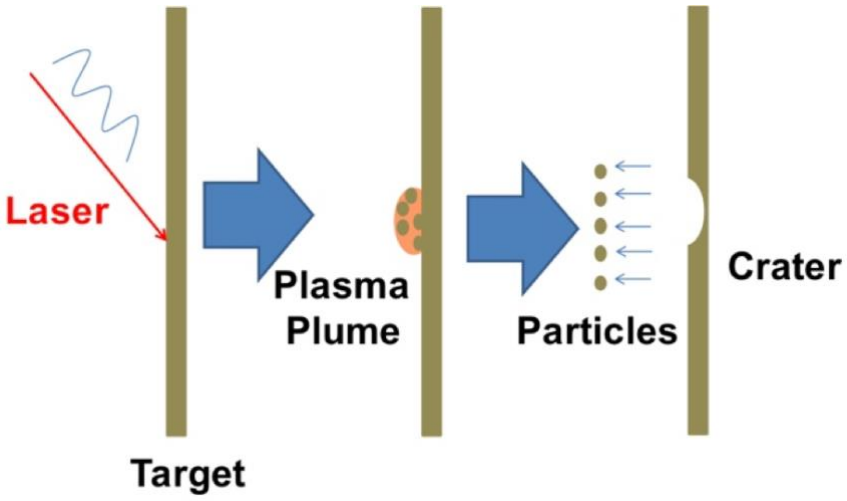

Figure 5. Physical mechanisms of generation of particles by PLA method.

The ejected material that experiences extreme pressure and temperature at very short interval time (ns), which now in disordered plasma state, is a highly reactive material. The liquid (CO_2) acts as the quenching agent is able to suppress the high-energy particles into more stable species. The scheme of this process is displayed in Fig. 6.

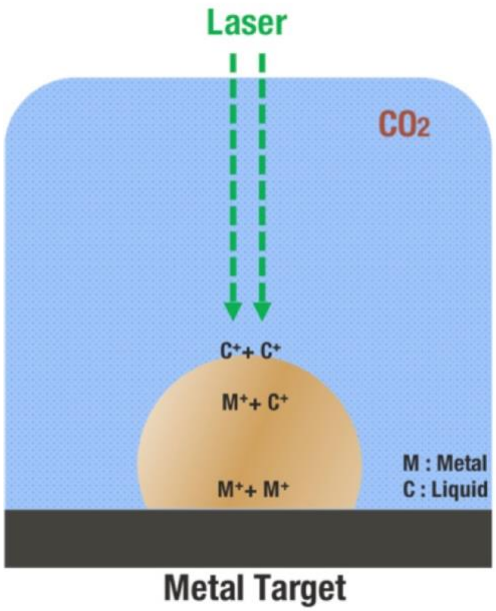

Figure 6. The schematic illustration of reaction between metal and liquid (CO_2) during PLA.

In the Au nanoparticle formation, Au remains in the neutral state since the oxidation of Au into its possible oxidized state, Au (III) require the Gibbs free energy of ca. 1300 kJ/mol [27]. The positive value of the Gibbs free energy means that the oxidation of Au into Au (III) is thermodynamically unfavorable. On the other hand, metal oxide nanoparticle can also be formed from the pristine metal, such as TiO_2 from Ti metal [28], apart that the oxidation of Ti into TiO_2 requires positive Gibbs free energy of ca. 500 kJ/mol [27]. This suggests that the work done to get the Gibbs free energy is provided by the energy of the incoming laser. The laser wavelength of 532 nm corresponds to the photon energy of 225 kJ/mol. It is reasonable to say that a two-photon adsorption likely occur on the oxidation of Ti. However, since the oxidation of Au into Au (III) requires larger amount of energy, the laser energy is probably not sufficient to oxidize Au.

The elemental analysis shows that the Au is covered by carbon network with the trace amount of oxygen on the surface. From the explanation above, it is unlikely that Au undergoes any redox reaction. Therefore, the most possible explanation is that the carbon atoms are covalently bond with each other to form large network of carbon nanostructures to cover the Au nanocluster similar to previous observation [15]. The dissociation energy of $CO_2 \rightarrow CO + O$ and $CO \rightarrow C + O$ are 525 and 1000 kJ/mol [29,31], respectively. The two-photon adsorption can occur under near critical and critical phase of CO_2 [30]. It is likely that CO_2 molecules dissociation reaction into CO + O is the initiation reaction. Furthermore, these reactive species induce chain reaction with other CO_2 or themselves to form carbon matrix covering the Au nanoparticles. The O atoms can oxidize the carbon since O can still be covalently bound to the sp2 amorphous carbon type nanostructure. The carbon matrix inhibits the growth of Au nanoparticles. Amendola et al. observed similar type of carbon-covered Au nanoparticles when pristine Au metal was irradiated in toluene [14]. It can be presumed that similar type of Au nanoparticles can be generated using PLA technique under organic solvent [32]. However, it is well known that most of organic solvents are toxic and expensive. Therefore, the synthesis of Au-carbon (Au-C) via laser ablation of Au in liquid and supercritical CO_2 can be an alternative method to synthesize this type of nanomaterial. The Au-C composite has potential application as sensor [33].

4-4 Conclusion

Au nanoparticles with carbon were successfully synthesized using the PLA method under supercritical CO_2. The PLA was carried out at temperatures of 40-80 °C,

pressure of 8–15 MPa and an irradiation time 15 min. The generated nanoparticles were characterized using a STEM system equipped with EDS. SEM images exhibited generated metal nanoparticles with spherical and nanocluster morphologies. The network structure of smaller metal nanoclusters appears to surround the larger metal nanoparticles. Au, C, and O were found to be uniformly distributed on the generated nanoclusters. The smallest size of the generated nanoparticles is expected to be obtained at CO_2 medium under the condition of temperature and pressure of 60 °C and 12 MPa, respectively. The results suggest that this method enables obtaining advanced nanostructured materials.

4-5 References:

[1] Bond G.C., Louis C. and Thompson D.T. 2006. Catalysis by Gold. Imperial College Press, London.

[2] Louis C and Pluchery O. 2012. Gold Nanoparticles for Physics. Chemistry and Biology. Imperial College Press, London.

[3] Ashkarran A. A. et al. 2009. Rapid and Efficient Synthesis of Colloidal Gold Nanoparticles by Arc Discharge Method. Appl. Phys. A. 96 (2): 423–428.

[4] Zeng H. et al. 2012. Nanomaterials via Laser Ablation/irradiation in Liquid: A Review, Adv. Funct. Mater. 22 (7): 1333–1353.

[5] Petersen S. et al. 2011. Penetratin-Conjugated Gold Nanoparticles-Design of Cell-Penetrating Nanomarkers by Femtosecond Laser Ablation. J. Phys. Chem. C. 115 (12): 5152–5159.

[6] Mafuné F. et al. 2001. Formation of Gold Nanoparticles by Laser Ablation in Aqueous Solution of Surfactant. J. Phys. Chem. B. 105 (22): 5114–5120.

[7] Sylvestre J. et al. 2004. Surface Chemistry of Gold Nanoparticles Produced by Laser Ablation in Aqueous Media. J. Phys. Chem. B. 108 (43): 16864–16869.

[8] Kabashin A. V. and Meunier M. 2003. Synthesis of Colloidal Nanoparticles during Femtosecond Laser Ablation of Gold in Water. J. Appl. Phys. 94 (12): 7941–7943.

[9] Besner S., Kabashin A. V. and Meunier M. 2007. Two-Step Femtosecond Laser Ablation-Based Method for the Synthesis of Stable and Ultra-Pure Gold Nanoparticles in Water. Appl. Phys. A Mater. Sci. Process. 88 (2): 269–272.

[10] Compagnini G. et al. 2007. Laser Synthesis of Au/Ag Colloidal Nano-Alloys: Optical Properties, Structure and Composition. Appl. Surf. Sci. 254 (4): 1007–1011.

[11] Compagnini G., Scalisi A. A. and Puglisi O. 2003. Production of Gold Nanoparticles by Laser Ablation in Liquid Alkanes. J. Appl. Phys. 94 (12): 7874–7877.

[12] Amendola V., Polizzi S. and Meneghetti M. 2006. Laser Ablation Synthesis of Gold Nanoparticles in Organic Solvents. J. Phys. Chem. B. 110 (14): 7232–7237.

[13] Nikov R. G. et al. 2017. Laser-Assisted Fabrication and Size Distribution Modification of Colloidal Gold Nanostructures by Nanosecond Laser Ablation in Different Liquids. Appl. Phys. A Mater. Sci. Process., 123 (7): 1–10.

[14] Amendola V. et al. 2005. Synthesis of Gold Nanoparticles by Laser Ablation in Toluene: Quenching and Recovery of the Surface Plasmon Absorption. J. Phys. Chem. B. 109 (49): 23125–23128.

[15] Mardis M., Wahyudiono, Takada N., Kanda H. and Goto M. 2018. Formation of Au-Carbon Nanoparticles by Laser Ablation under Pressurized CO2, Asia-Pacific J. Chem. Eng. e2176.

[16] Machmudah S., Wahyudiono, Takada, N., Kanda H., Sasaki K. and Goto M. 2013. Fabrication of Gold and Silver Nanoparticles with Pulsed Laser Ablation under Pressurized CO_2. Adv. Nat. Sci. Nanosci. Nanotechnol. 4 (4): 45011.

[17] Mardis M., Takada N., Machmudah S., Wahyudiono, Sasaki K., Kanda H. and Goto M. 2016. Nickel Nanoparticles Generated by Pulsed Laser Ablation in Liquid CO_2. Res. Chem. Intermed. 42 (5): 4581–4590.

[18] Machmudah S., Goto M., Wahyudiono, Kuwahara Y. and Sasaki M. 2011. Gold Nanoparticles Fabricated by Pulsed Laser Ablation in Supercritical CO_2. Res. Chem. Intermed. 37 (2–5): 515–522.

[19] Machmudah S., Sato T., Kuwahara Y., Sasaki M. and Goto M. 2011. Nano-Structured Material Fabrication Using Pulsed Laser Ablation in Supercritical CO_2, Trans. Mater. Res. Soc. Japan. 36 (3): 465–468.

[20] Machmudah S., Wahyudiono, Kuwahara Y., Sasaki M. and Goto M. 2011. Nano-Structured Particles Production Using Pulsed Laser Ablation of Gold Plate in Supercritical CO_2. J. Supercrit. Fluids. 60: 63–68.

[21] Machmudah S., Sato T., Wahyudiono, Sasaki M. and Goto M. 2012. Silver Nanoparticles Generated by Pulsed Laser Ablation in Supercritical CO_2 Medium, High Press. Res. 32 (1): 60–66.

[22] Kulinich S. A., Kondo T., Shimizu Y. and Ito T. 2013. Pressure Effect on ZnO Nanoparticles Prepared via Laser Ablation in Water. J. Appl. Phys. 113: 33509.

[23] Soliman W., Takada N., Koshizaki N. and Sasaki K. 2013. Structure and Size Control of ZnO Nanoparticles by Applying High Pressure to Ambient Liquid in Liquid-Phase Laser Ablation. Appl. Phys. A Mater. Sci. Process. 110 (4): 779–783.

[24] Koizumi M., Kulinich S. A., Shimizu Y. and Ito T. 2013. Slow Dynamics of Ablated Zone Observed around the Density Fluctuation Ridge of Fluid Medium. J. Appl. Phys. 114: 214301.

[25] Overschelde O. Van, Guisbiers G. and Wautelet M. 2009. Nanocrystallization of Anatase or Rutile TiO_2 by Laser Treatment. J. Phys. Chem. C 113 (34): 15343–15345.

[26] Van Overschelde O., Guisbiers G. and Snyders R. 2013. Green Synthesis of Selenium Nanoparticles by Excimer Pulsed Laser Ablation in Water. APL Mater. 1 (4).

[27] Lide D. R. 2003. CRC Handbook of Chemistry and Physics. 84th ed. CRC Press. Boca Raton, FL.

[28] Hajiesmaeilbaigi F., Motamedi A. and Ruzbehani M. 2009. Synthesis and Characterization of Composite Au/TiO_2 Nanoparticles by Laser Irradiation. Laser Phys. 20 (2): 508–511.

[29] Mellinger A. and Vidal C. R. 1995. Laser-Reduced Fluorescence Detection of Carbon Monoxide Npσ (N = 5–8) Triplet Rydberg States. Chem. Phys. Lett. 238 (1): 31–36.

[30] Fukuda T. et al. 2007. Dissociation of Carbon Dioxide and Creation of Carbon Particles and Films at Room Temperature. New J. Phys. 9.

[31] Matsumi Y. et al. 1991. Doppler Profiles and Fine-structure Branching Ratios of O(3Pj) from Photodissociation of Carbon Dioxide at 157 nm. J. Chem. Phys. 95 (10): 7311–7316.

[32] Amendola V. and Meneghetti M. 2009. Laser Ablation Synthesis in Solution and Size Manipulation of Noble Metal Nanoparticles. Phys. Chem. Chem. Phys. 11 (20): 3805.

[33] Simm A. O. et al. 2005. A Comparison of Different Types of Gold-Carbon Composite Electrode for Detection of arsenic(III). Anal. Bioanal. Chem. 381 (4): 979–985.

[CHAPTER 5]

Preparation of Gold Nanoparticles by Pulsed Laser Ablation in Glycine and L-proline

Abstract

This work presents a study of recent progress in laser ablation of metal in liquid medium for the synthesis of gold nanoparticles and its application. Glycine (Gly) and L-proline (Pro) solutions were used as a liquid medium for synthesized gold nanoparticles by pulsed laser ablation (PLA) process with 532 nm of fundamental wavelength at 1.84 mJ for 30 min. The generated particles were dispersed in glycine and L-proline solution and were analyzed by UV-vis spectroscopy and transmission electron microscopy (TEM). The influence of amino acids as a liquid medium and the possible mechanisms of particles formation are discussed

5-1 Introduction

Gold nanoparticle (Au-NP) is one of the most studied nanoparticle materials since it can be applied in wide array of fields, from chemistry to medical sciences [1–3]. The main advantage of Au-NPs is the availability of Au-NPs with controllable particle size and shape that can be obtained with appropriate synthetic methods. For example, Au-NPs particle size is controllable via synthesis route of chemical reduction of gold ions in solution [4,5]. However, the common synthetic routes of Au-NPs require vast amount of chemical reagents and produce undesired byproducts. Thus, the byproducts

and the excessive chemical reagents pose serious problems to the generated Au-NPs since they can reduce the purity of the Au-NPs [6].

An emerging synthesis method of nanoparticles within the last decade comes from the utilization of laser technology to produce nanoparticles, in particular generation of metal nanoparticles in liquid medium [7–10]. This laser-assisted NPs synthetic method proves to be comparable with the common chemical synthetic method in the term of the generated NPs. For instance, many studies revealed that it is possible to control the size of the produced metal nanoparticles. This can be conducted by varying the laser energy and the type and condition of the media [11–16].

In addition of the controllable generated NPs particle size, the laser ablation synthetic method can also generate some exotic NP phases that may not be obtained via common chemical synthetic methods. For example, crystalline titanium nitride (Ti_3N_4) NPs can be synthesized by irradiating titanium plate in liquid nitrogen [17]. Also, hybrid Zn/ZnO core/shell structure NPs can be generated by irradiating pristine zinc plate in an aqueous solution with sodium dodecyl sulfate (SDS) as the solute [18].

There have been plenty of reports on the laser ablation method to produce Au-NPs from Au plate immersed in pure liquid media such as water [19–22], n-decane [23], dimethylsulfoxide (DMSO), tetrahydrofuran (THF), acetonitrile (ACN) [24], chloroform [25], ethanol [25] and toluene [25,26]. Accordingly, the synthesis of Au-NPs via laser ablation in aqueous solution has also been explored. From literature, there have been reports on the generation of Au-NPs via laser ablation method in surfactant [27–29], inorganic salt and base [30], up to macromolecules such as cyclodextrin [31] and PAMAM G5 [32].

It is just recently that Au-NPs generated in amino acid solution gains attention. Haghighi et al. generated Au-NPs in 3,4-dihydroxyphenylalanine (DOPA) [33] solution. They showed that the generated Au-NPs are protected by a layer DOPA. This Au-DOPA complex exhibit high colloidal stability for a long period of time at room temperature and it is possible to enhance the cytotoxic activity of the amino acid against the Jurkat T-cells due to the presence of the Au NPs. The idea is that since proteins in cells consist of amino acids, there should be any interaction between the unique phases of the generated NPs with the amino acids to regulate the cell activity. Thus, opening the possibility to efficient drug design. Motivated by this intriguing discovery, we preliminarily report the results synthesis and characterization of Au-NPs in glycine and L-proline solution via laser ablation. Both amino acids play important role in cell regulation. Thus, interaction between Au-NPs and the amino acids can play important role to understand the role of Au in cells.

5-2 Experimental

5-2-1 Materials

A gold plate with an area of 1.5 × 1.5 cm and 1 mm of thick was purchased from Nilaco Co., Japan (purity: 99.95%). Water, glycine and L-prolyne were used as PLA medium was supplied by Sigma-Aldrich, Japan.

5-2-2 Experimental Setup and Procedures

Figure 1 depicts schematic of our laser ablation system consisting of Nd: YAG laser and a glass containing gold target immersed in aqueous solution.

Laser pulses from a high-power Q-switched pulsed Nd:YAG laser (Spectra-Physics Quanta-Ray INDI-40-10) with wavelength of 532 nm, pulse energy of 1.84 mJ, pulse

rate of 10 Hz, and pulse duration of approximately 8 ns, were used for ablation. A schematic of the PLA system for generating nanoparticles in amino acids is shown in Fig. 1. The gold target was immersed at the bottom of a beaker glass (300 mL volume) filled with an aqueous solution and the target was placed horizontally, approximately 1.5 m from Nd:YAG laser. A lens having a diameter of 20 mm (Sigma-Koki, Japan) was used to focus the laser beam onto the gold target. PLA was performed for 30 min for each medium (water, glycine solution, L-proline solution). All aqueous solutions used as ablation environment were prepared from deionized water. Water (99.99%), glycine (0.5M solution in water), L-prolyne (0.5M solution in water) were purchased from Sigma-Aldrich, Japan.

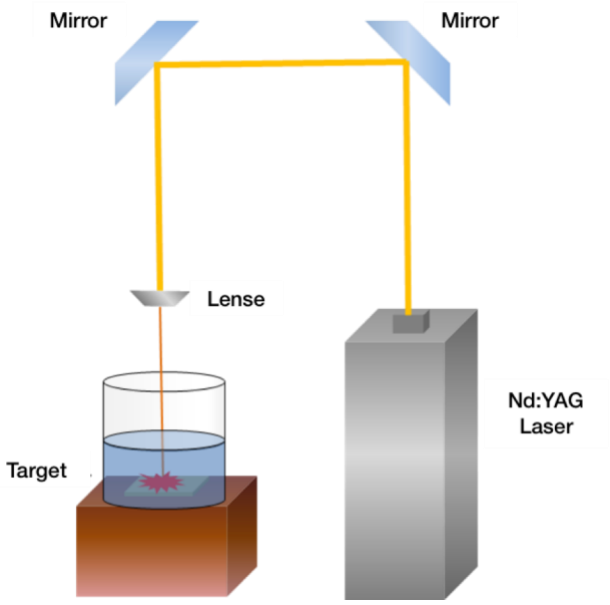

Figure 1. Schematic diagram of PLA experimental apparatus.

The generated particles were dispersed in solution (water, glycine and L-prolyne). The solution containing generated particles were analyzed by UV-vis made of Jasco, Japan.

The morphology of nanoparticles was studied using a high resolution transmission electron microscope (Hitachi H-800) equipped with a cold field-emission gun. The acceleration voltage was 200 kV, and the TEM images were captured by CCD (charge-coupled device) camera. The specimens were prepared by the following procedure: the sample was ultrasonically dispersed in ethanol for 15 min, then a drop of sample was loaded onto the copper grid and stored in desiccator overnight at room temperature to desorb atmospheric contaminants.

5-3 Results and Discussion

In order to know the effects of glycine and L-proline as a medium to produce Au-NPs, ablation was performed in 30 minutes under 3 different solutions (deionized water, 0.5 M glycine, 0.5 M L-proline). After ablation, generated particles were dispersed in each solution and analyzed by UV-vis (figure 2 and figure 3).

Figure 2 shows that the color of each solution after ablation was different as well as absorption spectra (figure 3). As we know, the size of Au-NPs determine the color we see. Dispersions of discrete gold nanoparticles in transparent media provide a fascinating range of colors, only recently exploited in the manufacture of paints and coatings. The gold particles in the amino acids (glycine and L-proline) on the middle and right are shown darker than generated Au-NPs in water. To the naked eye, the solution (Gly and Pro) has a red-dark color, instead of the red color characteristic of gold colloidal suspension. This phenomenon was similar with laser ablation in toluene or another aromatic solvent like benzonitrile. The solution`s color of aromatic solvent after ablation was yellow amber color and Amendola et al. explained that in some organic solvent the surface plasmon absorption (SPA) was not appeared [23].

Consequently, we suggested that generated Au-NPs in amino acids has different size. However, due to the lack of time and apparatus, the amounts of generated particles in this three solutions were not calculated yet.

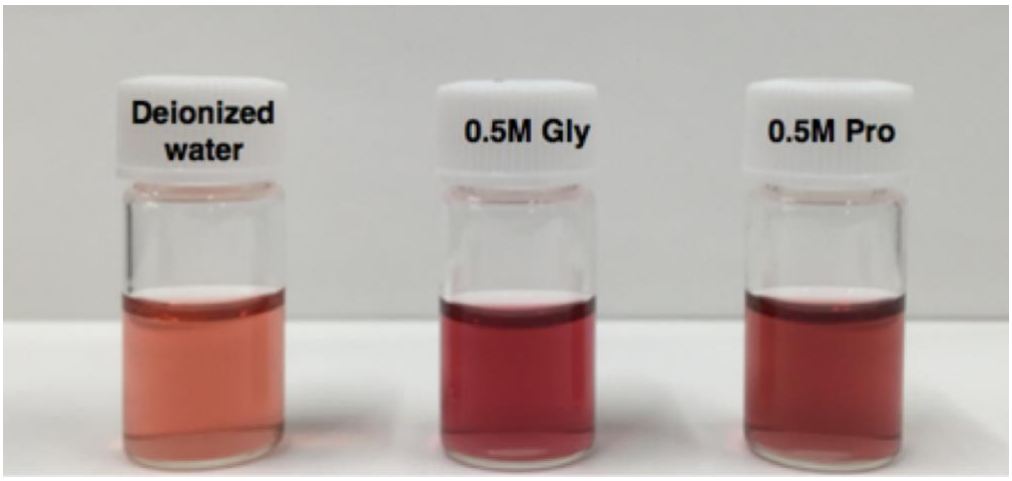

Figure 2. Au-NPs synthesis under doionized water, 0.5 M glycine, 0.5 M L-proline.

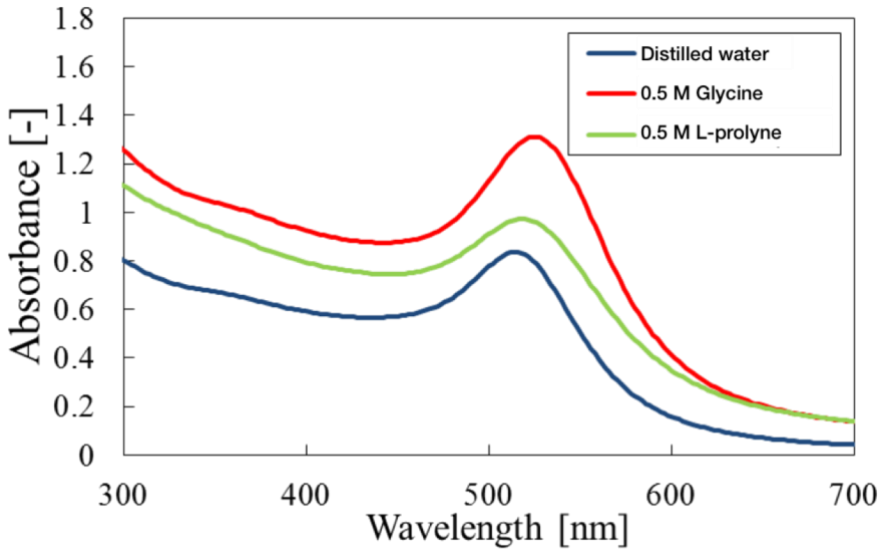

Figure 3. Absorption spectra of generated Au-NPs under water, 0.5M glycine, 0.5M L-proline.

Figure 3 shows absorption spectra of Au-NPs prepared at different ablation environments in the range of 300 to 700 nm. The curves show the absorption spectra that were prepared in water, 0.5 M glycine and 0.5 M L-proline. The absorption peaks were occurred at visible wavelengths, between 514 to 528 nm. Extinction absorption peaks of generated Au-NPs in water, 0.5 M glycine and 0.5 M L-proline were 514, 528 and 524 nm respectively, that can be assigned to the well-known surface plasmon resonance of sphere particles. Compared to deionized water, the extinction peak of Gly and Pro solution is higher than water and this result can be explained as follow. When the nanoparticles are formed by the liquid phase laser ablation method, on the surface of target material, plasma plume was formed. However, if an electrolyte is present around the solution, it would make easier for plasma plume to formed. Consequently, the plasma density will became higher so that the amount of particles generated is increased. Moreover, the extinction spectra of Au-NPs in Gly and Pro is slightly broader than in deionized water. Mie scattering theory explained that the wavelength of the maximum optical extinction and the shape of the spectra depends on the dielectric function of the medium, size, shape and material type of particles.

Shape and size of generated Au-NPs in amino acids were characterized by transmission electron microscope. The solution containing Au-NPs was dropped into carbon coated copper grids and let it dry completely at room temperature. Figure 4 shows a typical TEM image of Au-NPs prepared in 0.5 M Gly and Pro. As can be seen clearly, generated Au-NPs are spherical in shape so that we expected that slightly different of extinction peak of amino acids (Gly and Pro) is due to the different value of dielectric function of solutions. Dielectric constant of water is 80.4, while amino acids (Gly and Pro) are around 22.58~23.70. Moreover, no aggregation took place and the

size distribution is narrow with an average size is 7 nm for Au-NPs in Gly and 11 nm for Au-NPs in Pro.

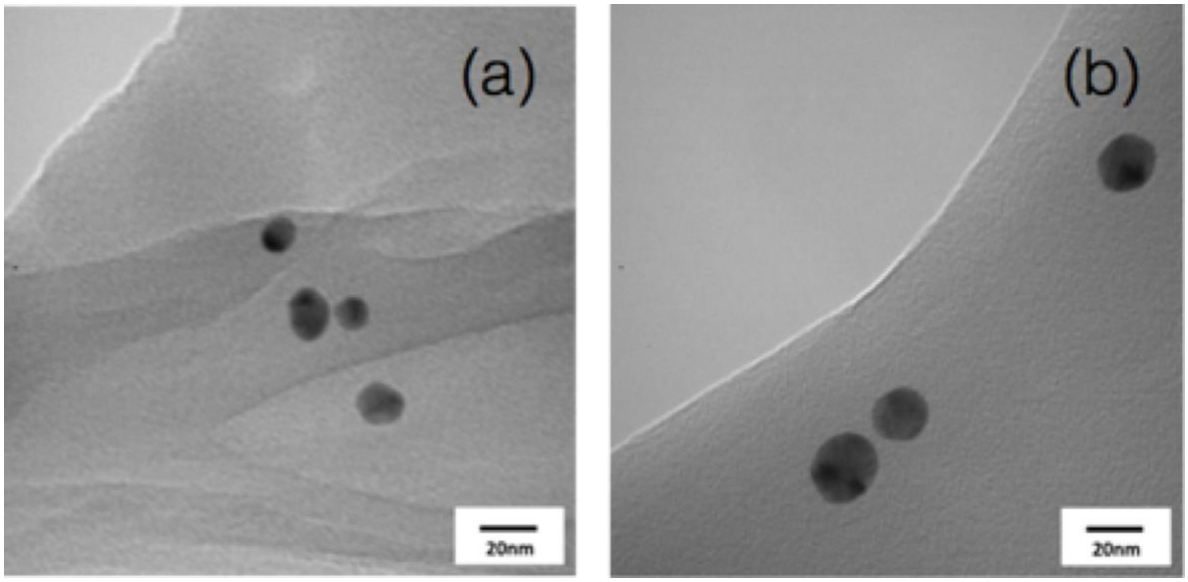

Figure 4. TEM images of Au-NPs generated in (a) 0.5M Gly and (b) 0.5M Pro.

In addition, in order to investigate the influences of amino acids (Gly and Pro) as a medium for laser ablation, after ablated in 30 minutes, Gly and Pro was removed from the solution by using dialysis membrane. Figure 5 shows the images solution before and after dialysis process.

From figure 5, it was confirmed that after dialysis process, the color of solution was change from red to blush-black color. This changing color was occurred due to surface plasmon resonance (SPR) that occurred when amino acid is removing, consequently, particles gradually aggregate as the concentration of amino acid decreased. It can be confirm also from the UV-vis absorption spectra (Figure 6 and 7). After removing amino acids from solution, not only the extinction peak was shift but also the absorption spectra was broadening in all wavelengths. Absorption extinction

spectra of metal nanoparticles have peaks at some wavelength due to surface plasmon resonance. The position of the peak is related to the size, shape and material type of nanoparticles. For spherical shape of particles, a single peak of extinction appears, while broadening of the spectra related to the size distribution and aggregation of particles [24].

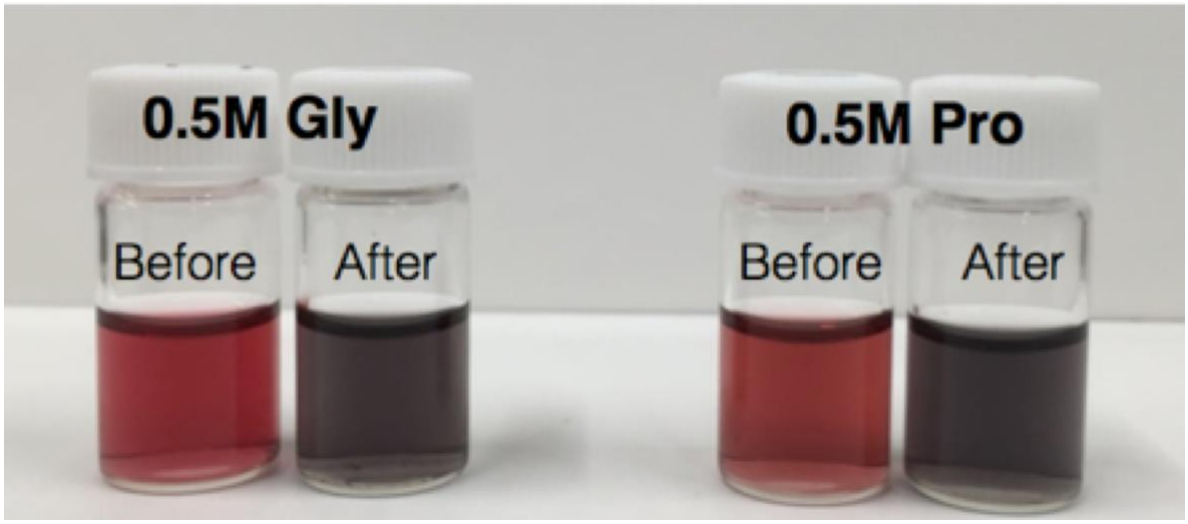

Figure 5. The images of 0.5 M Glycine and 0.5 M L-Prolyne after dialysis.

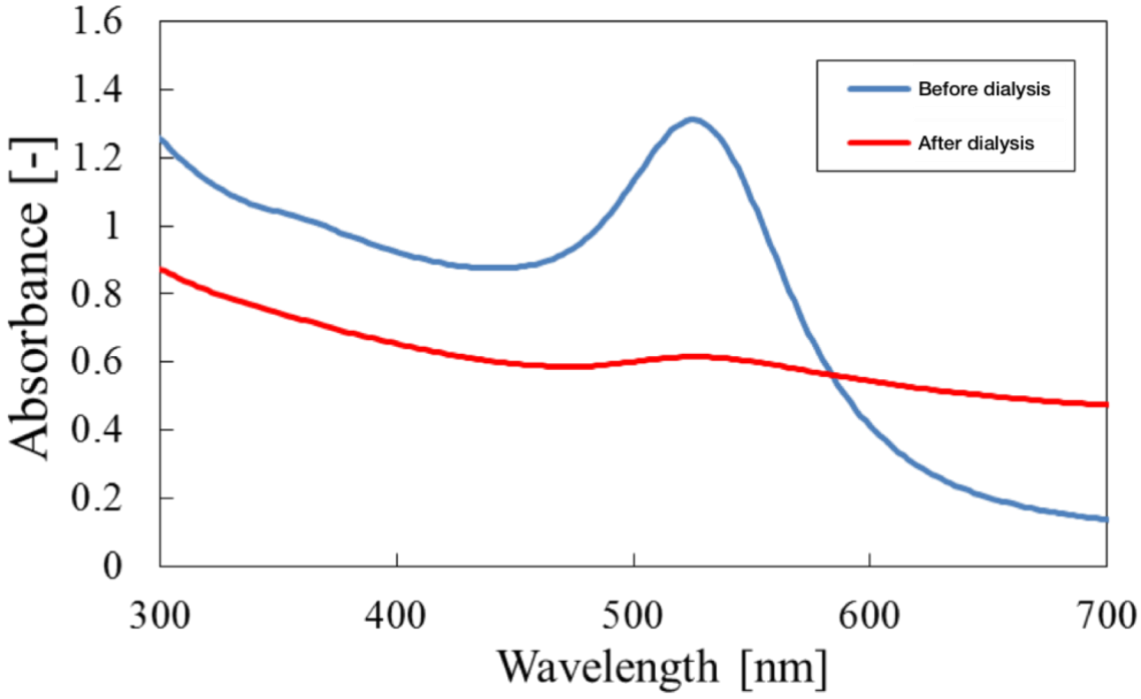

Figure 6. Absorption spectra of 0.5M glycine before and after dialysis.

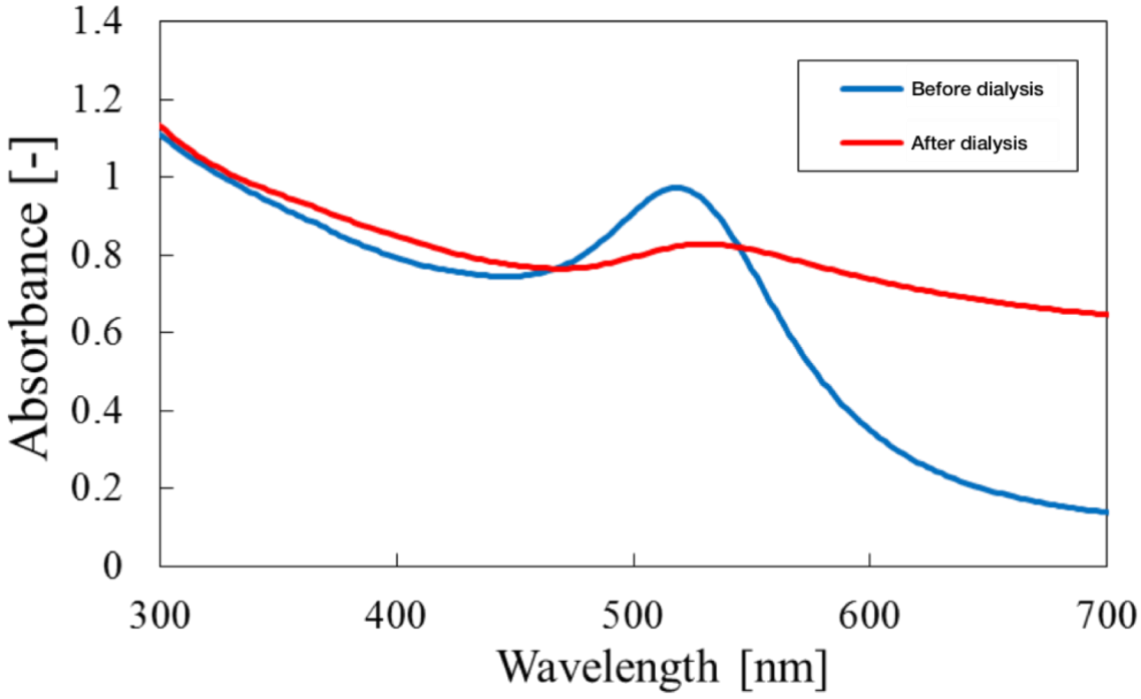

Figure 7. Absorption spectra of 0.5M L-proline before and after dialysis.

TEM images of Au-NPs after removing amino acids from the solution was shown in figure 8. The TEM images reported that Au-NPs was aggregated after amino acids (Gly and Pro) was removed. Au-NPs are clearly seen to spontaneously assemble into necklace or chain-like structure. It should be noted that no separate nanoparticle has been found, which reveals that Au colloidal particles prefer aggregation with each other than staying alone. Moreover, as shown in figure 8, every Au particle is closely linked with others and no gaps can be seen between particles. This finding method provides a new novel way for construction aggregation Au-NPs, which can be use in fabrication of single electron device.

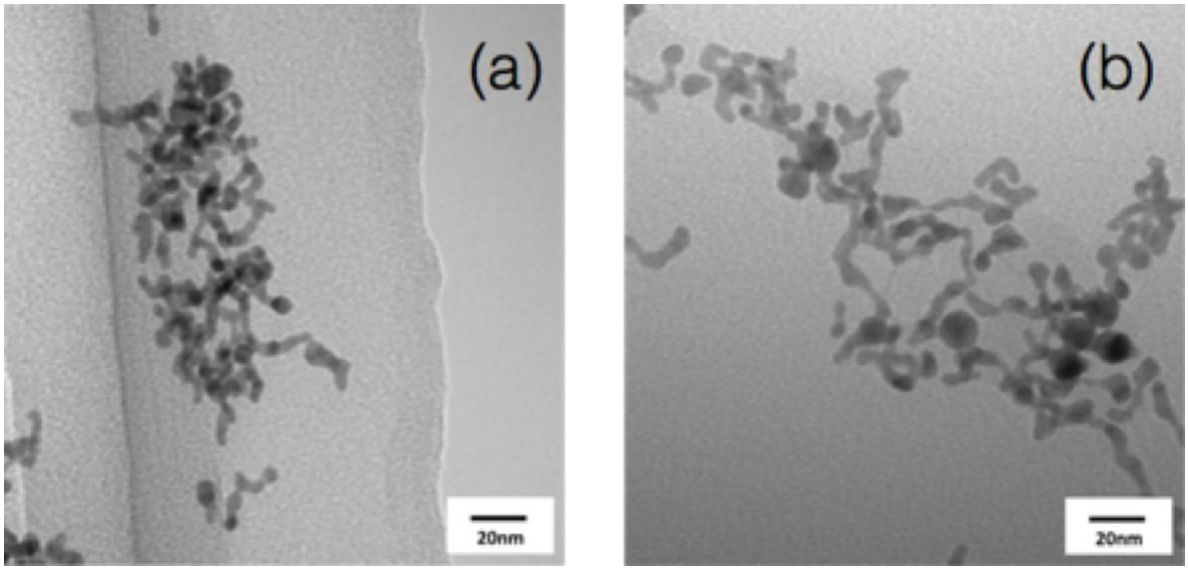

Figure 8. TEM images of Au-NPs generated in (a) 0.5M Gly and (b) 0.5M Pro after dyalisis

This formation of Au-NPs aggregation can be explained as follow. Due to the removing amino acids from solution, the concentration of amino acids is decreasing, which means the interaction of amino acid`s molecules is also decreased so that the

dipole-dipole interaction between gold particle each other become stronger. As a result, aggregation of particles is occurred. In addition, Tilaki et al [24] mentioned that in some solvents such as acetone, due to high dipole moment of surrounding moluecules, the overlapping of strong electrical double layers creates sufficient electrostatic repulsive force between particles. For this reason, no aggregation occurred.

5-4 Conclusion

By working with secondary harmony of pulsed laser ablation, we succeeded in producing small Au-NPs with narrow size distribution in Gly and Pro without any chemical agents. The effect of liquid medium on the size, optical properties and stability of Au-NPs were stuidied. Transmission electron microscope was used for characterization of the size and shape of generated particles. The generated Au-NPs was spherical shape in both solution, with an average size are 7 nm for Au-NPs in Gly and 11 nm for Au-NPs in Pro. Optical extinction spectra were also used to measure the optical properties of generated particles. A maximum optical extinction for generated Au-NPs in Gly and Pro are 528 and 524 nm, respectively. Dialysis was also performed in this work. After dialysis, generated Au-NPs was aggregated and formed chain-like structure. Optical extinction also shift and broadening with in all wavelength. Judging the results, high polar molecules like amino acid, provide strong surrounding electrical double layer, which can prevent nanoparticles to form aggregation.

5-5 References:

[1] M.C.M. Daniel, D. Astruc, Gold Nanoparticles: Assembly, Supramolecular Chemistry, Quantum-Size Related Properties and Applications toward Biology, Catalysis and Nanotechnology, Chem. Rev. 104 (2004) 293–346.

[2] P.K. Jain, K.S. Lee, I.H. El-Sayed, M.A. El-Sayed, Calculated Absorption and Scattering Properties of Gold Nanoparticles of Different Size, Shape, and Composition: Applications in Biological Imaging and Biomedicine, J. Phys. Chem. B. 110 (2006) 7238–7248.

[3] P. V. Kamat, Photophysical, Photochemical and Photocatalytic Aspects of Metal Nanoparticles, J. Phys. Chem. B. 106 (2002) 7729–7744.

[4] T. Yonezawa, T. Kunitake, Practical Preparation of Anionic Mercapto Ligand-Stabilized Gold Nanoparticles and Their Immobilization, Colloids Surfaces A Physicochem. Eng. Asp. 149 (1999) 193–199.

[5] K.J. Watson, J. Zhu, S.T. Nguyen, C.A. Mirkin, Hybrid Nanoparticles with Block Copolymer Shell Structures, J. Am. Chem. Soc. 121 (1999) 462–463.

[6] R.S. Sonawane, M.K. Dongare, Sol-Gel Synthesis of Au/TiO_2 thin Films for Photocatalytic Degradation of Phenol in Sunlight, J. Mol. Catal. A Chem. 243 (2006) 68–76.

[7] V. Amendola, M. Meneghetti, Laser Ablation Synthesis in Solution and Size Manipulation of Noble Metal Nanoparticles, Phys. Chem. Chem. Phys. 11 (2009) 3805.

[8] G.W. Yang, Laser Ablation in Liquids: Applications in the Synthesis of Nanocrystals, Prog. Mater. Sci. 52 (2007) 648–698.

[9] H. Zeng, X.W. Du, S.C. Singh, S.A. Kulinich, S. Yang, J. He, W. Cai, Nanomaterials via Laser Ablation/irradiation in Liquid: A Review, Adv. Funct. Mater. 22 (2012) 1333–1353.

[10] S. Barcikowski, F. Mafuné, Trends and Current Topics in the Field of Laser Ablation and Nanoparticle Generation in Liquids, J. Phys. Chem. C. 115 (2011) 4985.

[11] J.C. Alonso, R. Diamant, P. Castillo, M.C. Acosta-García, N. Batina, E. Haro-Poniatowski, Thin Films of Silver Nanoparticles Deposited in Vacuum by Pulsed Laser Ablation Using a YAG:Nd Laser, Appl. Surf. Sci. 255 (2009) 4933–4937.

[12] H. Imam, K. Elsayed, M.A. Ahmed, R. Ramdan, Effect of Experimental Parameters on the Fabrication of Gold Nanoparticles via Laser Ablation, Opt. Photonics J. 2 (2012) 73–84.

[13] S. Machmudah, T. Sato, Wahyudiono, M. Sasaki, M. Goto, Silver Nanoparticles Generated by Pulsed Laser Ablation in Supercritical CO_2 Medium, High Press. Res. 32 (2012) 60–66.

[14] S. Machmudah, M. Goto, Wahyudiono, Y. Kuwahara, M. Sasaki, Gold Nanoparticles Fabricated by Pulsed Laser Ablation in Supercritical CO_2, Res. Chem. Intermed. 37 (2011) 515–522.

[15] S. Wei, T. Yamamura, D. Kajiya, K.I. Saitow, White-Light-Emitting Silicon Nanocrystal Generated by Pulsed Laser Ablation in Supercritical Fluid: Investigation of Spectral Components as a Function of Excitation Wavelengths and Aging Time, J. Phys. Chem. C. 116 (2012) 3928–3934.

[16] T. Kato, S. Stauss, S. Kato, K. Urabe, M. Baba, T. Suemoto, K. Terashima, Pulsed Laser Ablation Plasmas Generated in CO_2 under High-Pressure Conditions up to Supercritical Fluid, Appl. Phys. Lett. 101 (2012) 224103.

[17] N. Takada, T. Sasaki, K. Sasaki, Synthesis of Crystalline TiN and Si Particles by Laser Ablation in Liquid Nitrogen, Appl. Phys. A Mater. Sci. Process. 93 (2008) 833–836.

[18] H. Zeng, Z. Li, W. Cai, B. Cao, P. Liu, S. Yang, Microstructure Control of Zn/ZnO Core/shell Nanoparticles and Their Temperature-Dependent Blue Emissions, J. Phys. Chem. B. 111 (2007) 14311–14317.

[19] S. Petersen, A. Barchanski, U. Taylor, S. Klein, D. Rath, S. Barcikowski, Penetratin-Conjugated Gold Nanoparticles - Design of Cell-Penetrating Nanomarkers by Femtosecond Laser Ablation, J. Phys. Chem. C. 115 (2011) 5152–5159.

[20] A. V. Kabashin, M. Meunier, Synthesis of Colloidal Nanoparticles during Femtosecond Laser Ablation of Gold in Water, J. Appl. Phys. 94 (2003) 7941–7943.

[21] S. Besner, A. V. Kabashin, M. Meunier, Two-Step Femtosecond Laser Ablation-Based Method for the Synthesis of Stable and Ultra-Pure Gold Nanoparticles in Water, Appl. Phys. A Mater. Sci. Process. 88 (2007) 269–272.

[22] G. Compagnini, E. Messina, O. Puglisi, V. Nicolosi, Laser Synthesis of Au/Ag Colloidal Nano-Alloys: Optical Properties, Structure and Composition, Appl. Surf. Sci. 254 (2007) 1007–1011.

[23] G. Compagnini, A.A. Scalisi, O. Puglisi, Production of Gold Nanoparticles by Laser Ablation in Liquid Alkanes, J. Appl. Phys. 94 (2003) 7874–7877.

[24] V. Amendola, S. Polizzi, M. Meneghetti, Laser Ablation Synthesis of Gold Nanoparticles in Organic Solvents, J. Phys. Chem. B. 110 (2006) 7232–7237.

[25] R.G. Nikov, N.N. Nedyalkov, P.A. Atanasov, D.B. Karashanova, Laser-Assisted Fabrication and Size Distribution Modification of Colloidal Gold Nanostructures by Nanosecond Laser Ablation in Different Liquids, Appl. Phys. A Mater. Sci. Process. 123 (2017) 1–10.

[26] V. Amendola, G.A. Rizzi, S. Polizzi, M. Meneghetti, Synthesis of Gold Nanoparticles by Laser Ablation in Toluene: Quenching and Recovery of the Surface Plasmon Absorption, J. Phys. Chem. B. 109 (2005) 23125–23128.

[27] F. Mafuné, J. Kohno, Y. Takeda, T. Kondow, H. Sawabe, Formation of Gold Nanoparticles by Laser Ablation in Aqueous Solution of Surfactant, J. Phys. Chem. B. 105 (2001) 5114–5120.

[28] M.A. Sobhan, M.J. Withford, E.M. Goldys, Enhanced Stability of Gold Colloids Produced by Femtosecond Laser Synthesis in Aqueous Solution of CTAB, Langmuir. 26 (2010) 3156–3159.

[29] A. Essaidi, M. Chakif, B. Schöps, A. Aumman, S. Xiao, C. Esen, A. Ostendorf, Size Control of Gold Nanoparticles during Laser Ablation in Liquids with Different Functional Molecules, J. Laser Micro Nanoeng. 8 (2013) 131–136.

[30] J. Sylvestre, S. Poulin, A. V Kabashin, E. Sacher, M. Meunier, J.H.T. Luong, Ä.P. De Montre, C. Postale, Surface Chemistry of Gold Nanoparticles Produced by Laser Ablation in Aqueous Media, J. Phys. Chem. B. 108 (2004) 16864–16869.

[31] A. V. Kabashin, M. Meunier, C. Kingston, J.H.T. Luong, Fabrication and Characterization of Gold Nanoparticles by Femtosecond Laser Ablation in an Aqueous Solution of Cyclodextrins, J. Phys. Chem. B. 107 (2003) 4527–4531.

[32] E. Giorgetti, A. Giusti, S.C. Laza, P. Marsili, F. Giammanco, Production of Colloidal Gold Nanoparticles by Picosecond Laser Ablation in Liquids, Phys. Status Solidi. 204 (2007) 1693–1698.

[33] F. Hajareh Haghighi, H. Hadadzadeh, H. Farrokhpour, Z. Amirghofran, S.Z. Mirahmadi-Zare, Stabilization of DOPA Zwitterions on Laser-Generated Gold Nanoparticles: ONIOM Computational Study of the Charge-Dependent Structural and Electronic Changes of DOPA Adsorbed on the Gold Nanosurface, J. Phys. Chem. C. 122 (2018) 8680–8692.

[CHAPTER 6]

In Situ Synthesis of Composite Au/TiO_2 Nanoparticles by Pulsed Laser Ablation in Water

Abstract

A novel synthetic approach of composite Au/TiO_2 nanoparticles has been developed with Pulsed Laser ablation (PLA) method. Gold (Au) and titania (TiO_2) nanoparticles were synthesized separetely in distilled water by ablating Au and Ti plate. The generated solution was dried into titanium plate at 200^oC. Then the coated titanium plate was immersed in distilled water and irradiated by Nd:YAG laser with 1064 nm laser beam for 50 seconds. The generated nanoparticles were characterized with field emission scanning electron microscopy (FE-SEM), transmission electron microscopy (TEM) and ultraviolet visible spectroscopy. From FE-SEM and TEM images, it was seen that the generated particles were spherical in shape with small Au particles attached into big TiO_2 particles, with particle sizes about 5-20 nm and 150-200 nm for Au and TiO_2 particles, respectively. Electron diffraction pattern, energy dispersive spectroscopy (EDS) and high resolution TEM (HRTEM) was also performed to qualify the generated particles. Furthermore, plausible mechanisms of formation composite particles were also discussed. Based on the results, this new method can also be used to obtain advanced nano-composite materials.

6-1 Introduction

Gold (Au) nanoparticle deposited on titania (TiO_2) nanosystem, dubbed as Au/TiO_2 composite nanoparticles show promising application in the daily life. For instance, its high photocatalytic [1] and antibacterial [2,3] activity properties are very useful to both convert the chemical pollutants into the less hazardous chemicals [4] and kill the harmful bacteria in water [2]. Hence, an efficient synthesis route of the Au/TiO_2 nanoparticles is one of the key components for mass-production of Au/TiO_2 nanoparticles for the aforementioned applications.

In conventional ways, Au/TiO_2 composite nanoparticles can be synthesized in several ways, such as by liquid phase route [3,5], combination of chemical reduction and sol-gel [6], combination of RF-sputtering and sol-gel [7], and hydrothermal [8]. However, most of these aforementioned methods are time consuming and require potentially environmentally harmful chemical reagents. Hence, an alternative rapid and facile synthetic method to produce composite Au/TiO_2 nanoparticles is required.

Nanomaterials synthesis via laser ablation/irradiation in liquid phase is one of the alternative methods to synthesize nanoparticles, in particular for Au/TiO_2. This method has been considered as a clean, facile and rapid way to synthesize the nanoparticles since it requires minimal amount of chemicals and also gives less byproducts and residues. Since laser has the strong ability to ablate many types of material, it can be used to produce almost any inorganic type nanomaterials including metals, oxides and sulfides, and among others. New phases of nanomaterials can be attained using this method where the other conventional methods usually fail [9].

While there have been many reports of the laser ablation method to individually produce TiO_2 nanoparticles [10-15] and Au nanoparticles [16-20] using the

laser ablation methods, there are still very few reports on synthesis of Au/TiO_2 composite nanoparticles [21,22]. Previously, Hajiesmailbaigi et al has successfully synthesized Au/TiO_2 nanoparticles by irradiating gold (Au) metal plate in TiO_2 sol solution with Nd:YAG laser at a wavelength of 1064 nm, a repetition rate of 5 Hz, and a pulse width of 20 ns [21]. The drawback of this method is that the preparation of TiO_2 sol still uses the conventional method, so it can take at least few hours to complete and requires many chemicals. Moslehirad et al [22] modified the preparation method of the TiO_2 by directly preparing the TiO_2 colloid from a pristine Ti metal immersed in distilled water using the laser ablation technique. A gold metal plate was then put into the TiO2 colloid and ablated using the same laser used to prepare TiO_2. In both cases, it was expected that the laser could assist the formation of the Au/TiO_2 nanoparticles from the "reaction" between TiO_2 and Au. However, most of the laser energy was adsorbed by the dispersed TiO_2 nanoparticles in the colloid, making the chance of the reaction between the precursor materials relatively small. This caused the small yield of the generated nanoparticles. Therefore, a way to enhance the reaction possibilities between the precursor components is urgently required.

In the present paper, we report an efficient and environmentally friendly synthetic method of Au/TiO_2 nanoparticles, in particular to increase the yield of generated nanoparticles, based on the combination of laser-assisted synthesis method described in the literatures [21-23] and our own proposed method using the pulsed laser ablation (PLA) method. Our proposed Au/TiO_2 nanoparticles synthesis method only requires both Au and Ti metal substrates and distilled water as the chemicals. We will show that our newly developed Au/TiO_2 nanoparticles synthesis method will yield considerably more Au/TiO_2 nanoparticles with good morphology compared to the

costly and chemically harmful methods and the previous laser-assisted synthesis methods.

6-2 Experimental

6-2-1 Materials

Gold and titanium plates with each area of 10 × 10 mm and a thickness of 1 mm were purchased from Nilaco Co., Japan (Ti purity: 99.5%, Au purity: 99.95%).

6-2-2 Experimental Setup and Procedure

Preparation of TiO_2 and Au solutions

The similar laser irradiation technique of synthesis of individual TiO_2 and Au in liquid from literatures [21-23] was used. To synthesize the TiO_2 (and Au) colloid solution, the titanium (and gold) plate was immersed at the bottom of a 30 ml beaker glass filled with 20 ml of distilled water and the target was placed horizontally, approximately 1.5 m from the laser. The system is then ablated with laser pulses from a high-power Q-switched pulsed Nd:YAG laser (Spectra-Physics Quanta-Ray INDI-40-10) with wavelength of 1064 nm, pulse energy of 19.0 J/cm^2, pulse rate of 10 Hz, and pulse duration of approximately 8 ns. A lens having a diameter of 20 mm (Sigma-Koki, Japan) was used to focus the laser beam onto the metal target. The schematic of the PLA system for generating nanoparticles is shown in figure 1. The system was ablated for 20 minutes. After the metal plate was ablated, the colloidal solution of Au and TiO_2 were formed, shown by the color change to red for Au and thin white for TiO_2, respectively. The Au and Ti metal plates were then dried and weighed to determine the concentration of the dispersed Au and TiO_2 nanoparticles in the water.

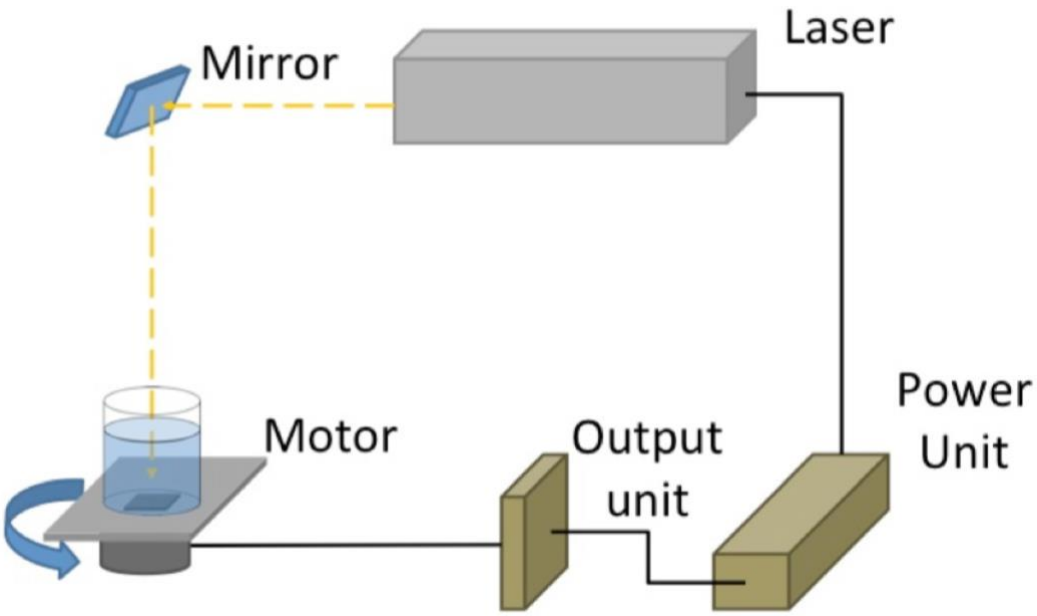

Figure 1. Schematics of PLA system. Signals are transmitted to motor and metal plate is rotated for each pulse to ablate new position. One rotation is about 50 seconds.

Synthesis of Au/TiO_2 composite nanoparticles

From previous works [21,22] we learned that the dispersed TiO_2 in the Au/TiO_2 colloidal solution may adsorb much of the laser energy, inhibiting the formation of Au/TiO_2 nanoparticles. Thus, we modified the treatment of both precursor materials as follows. Au and TiO_2 colloid solution were mixed and dried on titanium plate at 200^{o}C. This treatment causes the TiO_2 to be more concentrated on the titanium surface and in direct contact with Au. The Au/TiO_2 covered Ti plate was then immersed into distilled water and laser ablation was performed in 50 seconds. The generated particles were then dispersed in solution.

Characterization of Au/TiO_2 nanoparticles

To confirm the absorbance properties of composite nanoparticles, UV/Vis spectroscopy analysis was conducted using V-550 made by JASCO, Japan.

The morphologies of the generated nanoparticles were characterized by scanning electron microscopy (SEM) and transmission electron microscopy (TEM). SEM observation was performed by using a SU-8230 equipped with a cold field-emission gun made by Hitachi High-technologies with the sample dried onto silicon (Si) wafer. TEM observation was conducted using a JEM-2100F HK high-resolution transmission electron microscope (HR-TEM). The acceleration voltage was 200 kV, and the TEM images were captured by CCD (charge-coupled device) camera. The sample was ultrasonically dispersed in distilled water for 10 min, then a drop of sample was loaded onto the copper grid and stored in desiccator overnight at room temperature to desorb atmospheric contaminants. The specimens for TEM experiments were prepared by dropping solution containing generated particles onto micro copper grid (NP-C15) purchased by Okenshoji Co., Ltd and letting it dry completely at room temperature. The STEM sample specimens were prepared as the same procedure. STEM-EDS observations (Model JEM-2100F HK, JEOL, Japan) were also performed to determine the products elemental composition. The size of particles was measured by means of image analyzer software (Image J 1.42).

6-3 Results and Discussion

6-3-1 Morphological Studies

Applying PLA directly to the metal target eliminates the need for chemical precursors and enables generating clean nanoparticles. TEM images of the nanoparticles

generated by exposure to the Q-switched Nd:YAG pulsed laser beam are shown in figure 2. The morphology of generated particles was basically sphere-like structure.

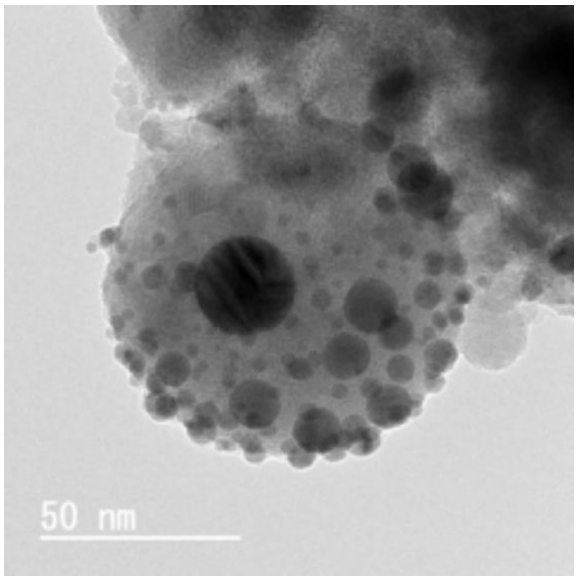

Figure 2. TEM images of generated Au/TiO_2 nanoparticles using PLA in distilled water.

As can be clearly seen, generated particles were spherical in shape with small particles attached into big particles, with particle sizes about 150 nm for big particles and 5-20 nm for attached gold particles (shown in figure 3).

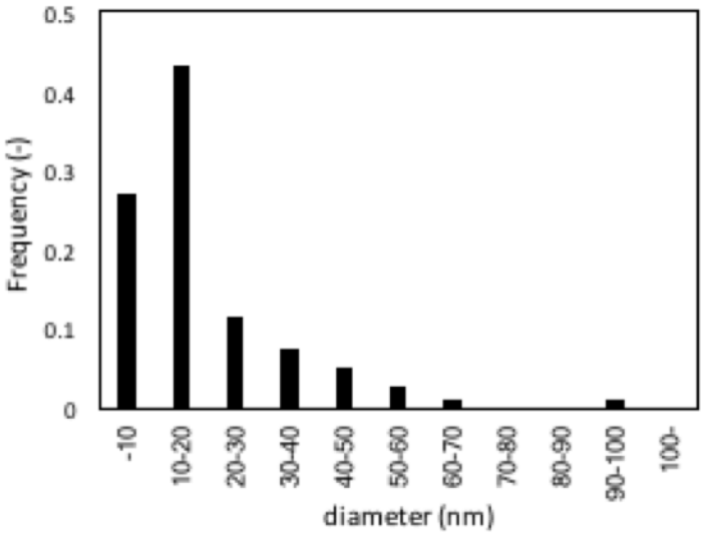

Figure 3. Size distribution of gold nanoparticles composed with TiO_2 measured by TEM.

Plasma, vapor, and nano/micro-sized molten metallic droplets could be generated as initial products when the pulsed laser beam was introduced to heat the metal target. These products then reacted with elements in the reaction medium to produce nanoparticles. Consequently, the generated metal nanoparticles consisted of spherical and nanocluster structures. We observed from figure 2 that there are two colors of generated particles, black and grey. Particles appearing more darken in TEM images are known to usually be metal particles. Accordingly, we examined the black color particles are gold and the grey particles are might be TiO_2 particles. Furthermore, to improve and clarify our observation, the SEM composition mapping imaging made with secondary and reflected electron image were conducted (figure 4).

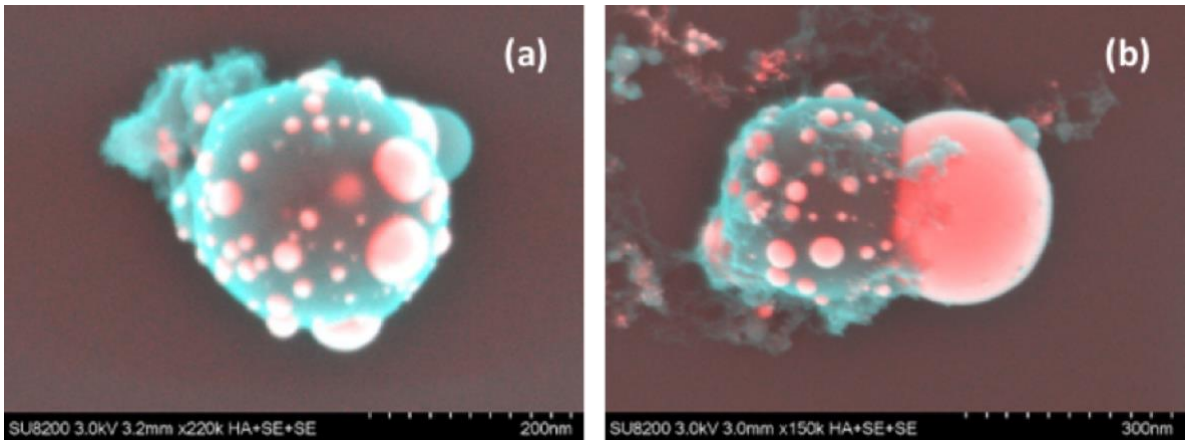

Figure 4. SEM images of generated Au/TiO_2 nanoparticles using PLA in distilled water. (Red: Au; Blue: Titanium)

Figure 4 shows clearly that both Au and Ti were detected. Since it is widely known SEM has poor resolution at extreme magnification, STEM observation for elemental composition mapping was conducted. Figure 5 shows the STEM-EDS elemental composition mapping images of generated Au/TiO_2 nanoparticles. As can be clearly observed, the big particle is contained titanium (Ti) and Oxygen (O) and small particles are gold (Au).

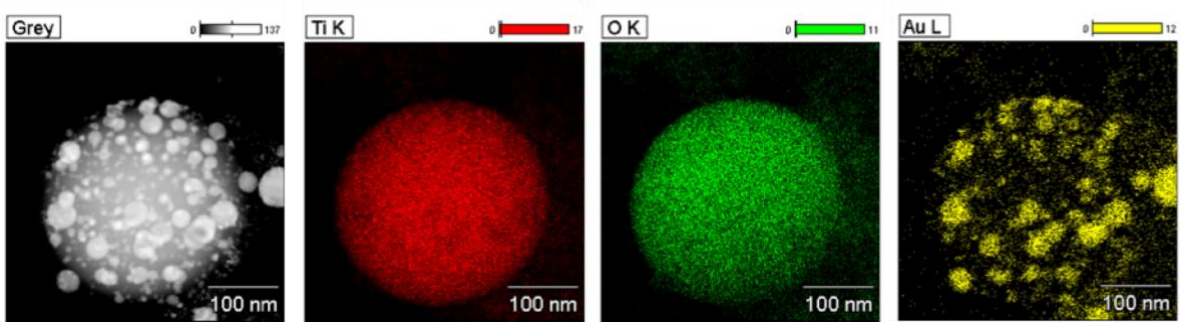

Figure 5. STEM-EDS elemental composition mapping images of generated Au/TiO_2 nanoparticles.

In order to make clear the composition of particles, UV-vis spectrum spectroscopy and TEM diffraction was conducted. It can be also clearly seen that the generated particles have both of Au and TiO_2 properties (figure 6 (a)) in absorbance spectrum. And the composite nanoparticles was found to be composed of anatase-type TiO_2 from TEM diffraction pattern (figure 6 (b)). The process of generation composite particles are discussed in next session.

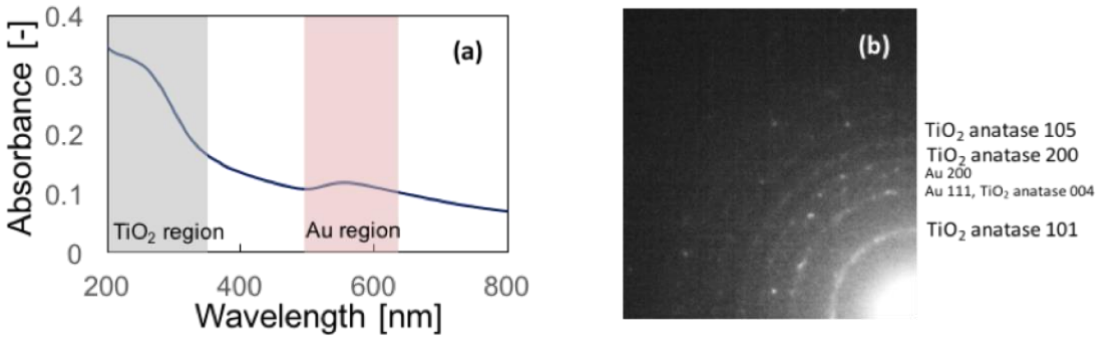

Figure 6(a). Characteristic absorbance and **6(b)**. Diffraction type of generated composite nanoparticles.

6-3-2 Plausible Mechanism of the Nanoparticles Formation

While the exact mechanism of laser induced nanoparticles formation is quite complex because the system is far from equilibrium [9] and no proper explanation has been deduced, the general physics behind nanomaterial creation via laser ablation can be simply viewed as the photon-electron, electron-electron and phonon-electron interactions [24]. In the first step of our experiment, the TiO_2 and the Au nanoparticles

were created from their respective metal. In both cases, the key point of the successful creation of the nanomaterial is the ability of the laser energy to eject some of the material from the bulk phases to the aqueous phases in order to form the nanoparticles. Due to laser interaction with the bulk material, further process can occur. The process includes heating, melting, ionization/vaporization and plasma creation. The ejected material experiences extreme pressure and temperature at very short interval time (ns). This will yield a highly reactive material, however the liquid (water) is able to quench these high-energy species into the stable species. In the case of TiO_2 formation, the titanium undergoes chemical reaction with water $Ti + 2H_2O \rightarrow TiO_2 + 2H_2$.

The Gibbs free energy of the reaction is ca. 500 kJ/mol [25], thus the reaction should not occur in the standard condition without any additional driving force, but in our case, the laser energy is able to add additional driving force for TiO_2 formation. In this case, we believe that the reactive Ti species collide with the surrounding water, creating the nanoparticles. In contrast with TiO_2, Au remains in the neutral state, because the reaction of gold with water to gold (III) oxide require ca. 1300 kJ/mol [25], much more positive compared to the Gibbs free energy of Ti oxidation reaction. The laser energy is probably not sufficient to oxidize Au. Therefore, the reaction between the high-energy Au and water are nearly negligible.

In the synthesis of the Au/TiO_2 composite, the mixture of previously dried Au and TiO_2 were put simultaneously on metal Ti plate in the distilled water, continued by the laser ablation. Our treatment of gold is different from the previous Au/TiO_2 laser assisted synthesis [21,22] where in previous works, the gold plate was immersed in the sol TiO_2 solution. It has been previously noted that during the laser irradiation, the laser that is adsorbed by the target has to travel through the liquid medium [24]. It implies

that the number of the pulse that reach the target depending on whether the light is reflected or adsorbed by the medium or not. In previous cases [21,22], we believe that much of the laser was either adsorbed or reflected by the TiO_2 in the medium, since it has blue color. On the other hand, in our case, the TiO_2 was readily deposited into the Ti plate along with the Au nanoparticle. This will minimize the dispersed TiO_2 in the solution. Since solution almost has no color, we can achieve more nanoparticle using less ablation energy, because more pulse can reach the target without being reflected or adsorbed by the medium.

The mechanism of Au/TiO_2 composite nanoparticle formation also involves heating, melting, ionization/vaporization and plasma creation. In nanoparticle, the melting temperature decreases with respect to the nanoparticle size following equation [26,27]

$$\frac{T_m}{T_{m,\infty}} = 1 - \frac{\alpha_{shape}}{2L} \quad (1)$$

where T_m, $T_{m,\infty}$, α_{shape} and L are the melting temperature of the nanoparticle, melting temperature of the bulk phase, shape constant and nanoparticle size, respectively. For spherical nanoparticle, L is the radius of the sphere. The α shape depends on the surface energy of the bulk phase and the fusion enthalpy of the bulk material. Figure 6(b) shows the electron diffraction of generated composite nanoparticles. For spherical TiO_2 (anatase) the shape constant is 1.27 [26] while for Au, the shape constant is 1.83 [27]. From the first ablation, we obtained the spherical nanoparticle for TiO_2 with size (diameter) of approximately 200 nm while for Au the size is approximately 20 nm. The melting temperature for bulk TiO_2 (anatase) and Au are 2075 and 1337 K [25],

respectively. From eq. (1), we obtain the melting point of the TiO_2 and Au nanoparticles approximately 2060 and 1210 K, respectively.

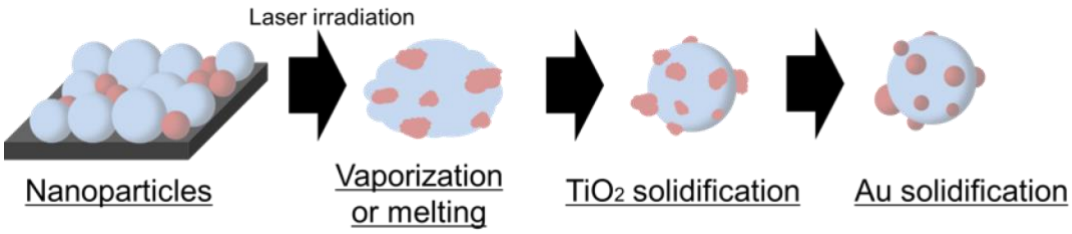

Figure 7. Plausible illustration mechanism of Au/TiO_2 composite nanoparticles formation.

As shown in figure 7, when the Au and TiO_2 composite were ablated, the laser energy was used to melt and probably vaporize the nanoparticles. The high temperature and pressure phase is then quenched by water into their equilibrium states. Since the melting point of Au is much lower than the melting point of TiO_2, even at the nanoscale, Au nanoparticles were melted earlier than TiO_2. This allows the small Au nanoparticles to diffuse freely on the solid TiO_2 surface. When TiO_2 melted, some of the larger TiO_2 broke into smaller TiO_2 nanoparticles while some of the melted Au still on its surface. Collision with water causes the melted nanoparticle to crystallize/solidify. In the crystallization process, TiO_2 solidify first followed by Au due to their differences in their melting temperature. The generated nanoparticles are generally spherical because the nucleation occurred in the water and expand their size in the direction where the pressure stress is minimal [28]. In the case of water or liquid in general, all directions in the space are equal. Therefore, the nanoparticles can have spherical shape in the water/liquid medium.

6-4 Conclusion

We have developed a facile and environmentally friendly method to synthesize Au/TiO_2 using pulsed laser ablation (PLA). The generated nanoparticles has spherical morphology with Au particles attached into TiO_2 particles with the average size of 5-20 nm and 100-150 nm, respectively. The mechanism of the nanoparticle formation has also been explained that composite nanoparticles were synthesized by the difference of melting point. Based on the results, our method can be used as an alternative method to synthesize Au/TiO_2 nanoparticles along with the conventional methods.

6-5 References

[1] H. Li, Z. Bian, J. Zhu, Y. Huo, H. Li, and Y. Lu, "Mesoporous Au/TiO_2 Nanocomposites with Enhanced Photocatalytic Activity", J. American Chem. Soc., vol. 129, pp. 4538–4539, Mar., 2007.

[2] L. Armelao, D. Barreca, G. Bottaro, A. Gasparotto, C. Maccato, C. Maragno, E. Tondello, U. L. Štangar, M. Bergant, and D. Mahne, "Photocatalytic and Antibacterial Activity of TiO_2 and Au/TiO_2 Nanosystems", Nanotechnology, vol. 18, pp. 375709, Aug., 2007.

[3] G. Fu, P. S. Vary, and C.-T. Lin, "Anatase TiO_2 Nanocomposites for Antimicrobial Coatings", J. Phys. Chem. B., vol. 109, pp. 8889–8898, Mar., 2005.

[4] A. Ayati, A. Ahmadpour, F. F. Bamoharram, B. Tanhaei, M. Mänttäri, and M. Sillanpää, "A Review on Catalytic Applications of Au/TiO_2 Nanoparticles in the Removal of Water Pollutant", Chemosphere, vol. 107, pp. 163–174, Feb., 2014.

[5] P. D. Cozzoli, M. L. Curri, C. Giannini, and A. Agostiano, "Synthesis of TiO_2-Au Composites by Titania-Nanorod-Assisted Generation of Gold Nanoparticles at Aqueous/Nonpolar Interfaces", Small, vol. 2, pp. 413–421, Jan., 2006.

[6] D. Buso, J. Pacifico, A. Martucci, and P. Mulvaney, "Gold-Nanoparticle-Doped TiO_2 Semiconductor Thin Films: Optical Characterization", Adv. Funct. Mater., vol. 17, pp. 347–354, Jan., 2007.

[7] L. Armelao, D. Barreca, G. Bottaro, A. Gasparotto, E. Tondello, M. Ferroni, and S. Polizzi, "Au/TiO_2 Nanosystems: A Combined RF-Sputtering/Sol-Gel Approach", Chem. Mater., vol. 16, pp. 3331–3338, Apr., 2004.

[8] J. Yu, L. Yue, S. Liu, B. Huang, and X. Zhang, “Hydrothermal Preparation and Photocatalytic Activity of Mesoporous Au-TiO_2 Nanocomposite Microspheres”, J. Colloid Interface Sci., vol. 334, pp. 58–64, Apr., 2009.

[9] H. Zeng, X. W. Du, S. C. Singh, S. A. Kulinich, S. Yang, J. He, and W. Cai, “Nanomaterials via Laser Ablation/Irradiation in Liquid: A Review”, Adv. Funct. Mater., vol. 22, pp. 1333–1353, 2012.

[10] A. S. Nikolov, P. A. Atanasov, D. R. Milev, T. R. Stoyanchov, A. D. Deleva, and Z. Y. Peshev, “Synthesis and Characterization of TiOx Nanoparticles Prepared by Pulsed-Laser Ablation of Ti Target in Water”, Appl. Surf. Sci., vol. 255, pp. 5351–5354, 2009.

[11] C. N. Huang, J. S. Bow, Y. Zheng, S. Y. Chen, N. J. Ho, and P. Shen, “Nonstoichiometric Titanium Oxides via Pulsed Laser Ablation in Water”, Nanoscale Res. Lett., vol. 5, pp. 972–985, Apr., 2010.

[12] A. Nath, S. S. Laha, and A. Khare, “Synthesis of TiO_2 Nanoparticles Via Laser Ablation at Titanium-Water Interface”, Integr. Ferroelectr., vol. 121, pp. 58–64, Apr., 2010.

[13] F. Tian, J. Sun, J. Yang, P. Wu, H. L. Wang, and X. W. Du, “Preparation and Photocatalytic Properties of Mixed-Phase Titania Nanospheres by Laser Ablation”, Mater. Lett., vol. 63, pp. 2384–2386, Nov., 2009.

[14] P. Liu, W. Cai, M. Fang, Z. Li, H. Zeng, J. Hu, X. Luo, and W. Jing, “Room Temperature Synthesized Rutile TiO_2 Nanoparticles Induced by Laser Ablation in Liquid and Their Photocatalytic Activity”, Nanotechnology, vol. 20, pp. 285707, June, 2009.

[15] S. M. Hong, S. Lee, H. J. Jung, Y. Yu, J. H. Shin, K.-Y. Kwon, and M. Y. Choi, "Simple Preparation of Anatase TiO_2 Nanoparticles via Pulsed Laser Ablation in Liquid", Bull. Korean Chem. Soc., vol. 34, pp. 279–282, Jan., 2013.

[16] S. Petersen, A. Barchanski, U. Taylor, S. Klein, D. Rath, and S. Barcikowski, "Penetratin-Conjugated Gold Nanoparticles-Design of Cell-Penetrating Nanomarkers by Femtosecond Laser Ablation", J. Phys. Chem. C., vol. 115, pp. 5152–5159, Dec., 2010.

[17] Mafuné Fumitaka, J. Kohno, Y. Takeda, T. Kondow, and H. Sawabe, "Formation of Gold Nanoparticles by Laser Ablation in Aqueous Solution of Surfactant", J. Phys. Chem. B., vol. 105, pp. 5114–5120, Feb., 2001.

[18] J. Sylvestre, S. Poulin, A. V Kabashin, E. Sacher, M. Meunier, J. H. T. Luong, Ä. P. De Montre, and C. Postale, "Surface Chemistry of Gold Nanoparticles Produced by Laser Ablation in Aqueous Media", J. Phys. Chem. B., vol. 108, pp. 16864–16869, July, 2004.

[19] A. V. Kabashin and M. Meunier, "Synthesis of Colloidal Nanoparticles During Femtosecond Laser Ablation of Gold in Water", J. Appl. Phys., vol. 94, pp. 7941–7943, Sep., 2003.

[20] S. Besner, A. V. Kabashin, and M. Meunier, "Two-Step Femtosecond Laser Ablation-Based Method for the Synthesis of Stable and Ultra-Pure Gold Nanoparticles in Water", Appl. Phys. A Mater. Sci. Process., vol. 88, pp. 269–272, May, 2007.

[21] F. Hajiesmaeilbaigi, A. Motamedi, and M. Ruzbehani, "Synthesis and Characterization of Composite Au/TiO_2 Nanoparticles by Laser Irradiation", Laser Phys., vol. 20, pp. 508–511, Dec., 2009.

[22] F. Moslehirad, M. H. Majles Ara, and M. J. Torkamany, “Synthesis of Composite Au/TiO_2 Nanoparticles Through Pulsed Laser Ablation and Study of Their Optical Properties”, Laser Phys., vol. 23, pp. 075601, May, 2013.

[23] D. M. Bubb, S. M. O’Malley, J. Schoeffling, R. Jimenez, B. Zinderman, and S. Yi, “Size Control of Gold Nanoparticles Produced by Laser Ablation of Thin Films in an Aqueous Environment”, Chem. Phys. Lett., vol. 565, pp. 65–68, Jan., 2013.

[24] O. Van Overschelde, G. Guisbiers, and R. Snyders, “Green Synthesis of Selenium Nanoparticles by Excimer Pulsed Laser Ablation in Water”, APL Mater., vol. 1, Oct., 2013.

[25] D. R. Lide, CRC Handbook of Chemistry and Physics, 84th Edition, CRC Press, Boca Raton, FL, 2003.

[26] G. Guisbiers, O. Van Overschelde, and M. Wautelet, “Theoretical Investigation of Size and Shape Effects on the Melting Temperature of TiO_2 Nanostructures”, Appl. Phys. Lett., vol. 92, pp. 103121, Mar., 2008.

[27] G. Guisbiers, M. Kazan, O. Van Overschelde, M. Wautelet, and S. Pereira, “Mechanical and Thermal Properties of Metallic and Semiconductive Nanostructures”, J. Phys. Chem. C., vol. 112, pp. 4097–4103, Nov., 2007.

[28] O. Van Overschelde, G. Guisbiers, and M. Wautelet, “Nanocrystallization of Anatase or Rutile TiO_2 by Laser Treatment”, J. Phys. Chem. C., vol. 113, pp. 15343–15345, July 2009.

[CHAPTER 7]

Summary and Future Plans

7.1 Summary

The merits of liquid phase laser ablation over other conventional methods for synthesizing nanoparticles attract the attention of many researchers in the field of nanotechnology. Understanding the synthesis dynamics of nanoparticles is very important to optimize and to control the size and the structure of nanoparticles. The fundamental investigations of growth processes of nanoparticle are seriously insufficient. Moreover, exploiting the liquid pressure to control the properties of nanoparticles in liquid–phase laser ablation is an absolutely new idea. Therefore, in the present study, firstly, we investigated the synthesis dynamics of nanoparticles by laser ablation in liquid and supercritical CO_2, in particular the place for the growth of nanoparticles. Secondly, we investigated the effect of the type of the liquid media on the synthesis dynamics of nanoparticles.

In chapter 2 we observed 3 types of particles by irradiating nickel target under liquid CO_2. These 3 types are nickel-rich particles, carbon-rich particles and nickel-carbon particles. Furthermore, the shape of generated particles was almost sphere shaped, apple-like shaped, core/shell shaped.

In chapter 3 and 4, we show that Au nanoparticles with carbon were successfully synthesized using the PLA method under pressurized and supercritical CO_2. We observed that generated Au-NPs were not standing alone as pure Au-NPs, but

instead a network structure of the smaller metal nanoclusters (Au-NPs) covered by the network of carbon nanostructure and the trace amount of oxygen larger metal nanoparticles.

In chapter 5 we succeeded in producing small Au-NPs with narrow size distribution in glycine and proline without any significant amount of chemical agents employing the secondary harmony of pulsed laser ablation. We demonstrate that the, high polar molecules like amino acid can prevent nanoparticles to form aggregation due to the electrical double layer provided.

In chapter 6, we have developed a facile and environmentally friendly method to synthesize Au/TiO_2 in water using pulsed laser ablation (PLA). The mechanism of the nanoparticle formation has also been explained that composite nanoparticles were generated by the difference of melting point.

7.2 Future Plans

We introduced theoretical explanation to study the dynamics of cavitation bubble in liquid phase laser ablation. However, the process of generation particles from plasma plume has not cleared yet, and as a result, we believe that generated cavitation bubble on the plasma plume has a significant effect to form shape and size of particles. Therefore, a more detailed of cavitation bubble experiment is necessary for understanding the effect of bubble. Moreover, because the role of density CO_2 has significant effect to the generated particles, a more detail investigation and experiment is highly recommended.

The lack theoretical investigation of laser ablation process is one of the key reasons why this process has not cleared yet. What controls the compounds, shape and size of

particles are necessary recommended to investigate. Not only CO_2, but also another fluid such as nitrogen, argon as a medium are worth to make investigation. Furthermore, the applications and properties of generated particles is also need to examine.

List of Publications

1) Mardianstah Mardis, Noriharu Takada, Siti Machmudah, Wahyudiono, Hideki Kanda, Motonobu Goto, Nickel nanoparticles generated by plused laser ablation in Liquid CO_2, Research on Chemical Intermediates, 42(5) 4581-4590, 2016.

2) Mardiansyah Mardis, Wahyudiono, Noriharu Takada, Hideki Kanda, Motonobu Goto, Formation of Au–Carbon Nanoparticles by Laser Ablation under Pressurized CO_2, Asia-Pacific Journal of Chemical Engineering, 13(2) e2176(1)-e2176(8), 2018.

3) Mardiansyah Mardis, Wahyudiono, Noriharu Takada, Hideki Kanda, Motonobu Goto, Consideration of Au–Carbon Nanoparticles by Laser Ablation under Supercritical CO_2, ARPN Journal of Engineering and Applied Sciences, 2018.

Acknowledgments

Firstly, I would like to express my sincere gratitude to my advisor Prof. Goto Motonobu for the continuous support of my doctoral study and related research, for his patience, motivation, and immense knowledge during my stay in Nagoya University. His guidance helped me in all the time of research and writing of this doctoral disertation. I could not have imagined having a better advisor and mentor for my doctoral study. Besides my advisor, I would like to thank to Dr. Hideki Kanda, not only because of his insightful comments and encouragement, but also for the hard question which incented me to widen my research from various perspectives. My sincere thanks also goes to Dr. Wahyudiono and Dr. Takada Noriharu, as a researcher in Nagoya University, who always taught me how to build apparatus from zero, write good paper, etc. Without their precious supports it would not be possible to conduct this research.